

Systematics of multilayer adsorption phenomena on attractive substrates

Rahul Pandit*

*Department of Physics and Materials Research Laboratory, University of Illinois at Urbana-Champaign,
Urbana, Illinois 61801*

M. Schick

Department of Physics, University of Washington, Seattle, Washington 98195

Michael Wortis

*Department of Physics and Materials Research Laboratory, University of Illinois at Urbana-Champaign,
Urbana, Illinois 61801*

(Received 25 May 1982)

This paper presents a systematic classification of multilayer-adsorption phenomena on attractive substrates, with emphasis on the buildup of thick films. The approach is based on statistical mechanics and includes adsorption-desorption effects and the interrelation of bulk and surface behavior. The surface phase diagram depends qualitatively on the relative strengths and ranges of adatom-adatom and adatom-substrate attractions. When the adatom-substrate attraction dominates (strong substrate), the film builds up uniformly, as the bulk adatom density increases, and the excess surface density diverges at coexistence (complete wetting). The buildup proceeds via an infinite sequence of discrete layer transitions (layering) at low temperatures (below the roughening temperature T_R) and smoothly at higher temperatures, as originally noted by de Oliveira and Griffiths. Substrates of intermediate strength are characterized by a wetting temperature T_W above which wetting at coexistence is complete but below which the film thickness builds up only to a finite value, as coexistence is approached. The relative values of T_W and T_R define three subregions: When $T_W < T_R$, layering occurs, with an infinite sequence of transitions between T_W and T_R ; when $T_R \lesssim T_W$, layer transitions have coalesced into a single thick-film—thin-film transition (prewetting); when $T_R \ll T_W$, prewetting may disappear, leaving only a critical-wetting transition on the coexistence axis. For still weaker substrates, wetting is incomplete at all temperatures; however, a variety of drying phenomena may occur on the high-density side of bulk coexistence. Specific calculations are given for a lattice-gas model at $T=0$ and in the mean-field approximation. Conclusions are informed, in addition, by certain exact results and symmetries. The last section includes a critical discussion of the relation of the lattice-gas model to the real world and a brief review of relevant experimental data.

I. INTRODUCTION

Over the past two decades a great variety of experiments have studied the process of physisorption on inert substrates and a fascinatingly rich phenomenology has emerged.¹⁻⁴ Much of this work was motivated by the desire to study strictly two-dimensional systems—particularly, perhaps, because of exciting theoretical advances in this area⁴—and focused on submonolayer phenomena. In this regime the attractive interaction which binds the adatoms to the substrate is very strong and the interesting physics, which takes place on energy

scales of order $k_B T$, is dominated by the lateral interactions, both adatom-adatom and adatom-substrate, which serve to determine the two-dimensional ordering. There is also, however, an accumulating body of experimental data probing the third dimension. This data, taken at higher bulk densities (i.e., nearer bulk coexistence), has attracted much less theoretical attention and forms the object of our study.

Beyond the first few monolayers substrate interaction fall off rapidly (roughly as z^{-3} for van der Waals forces, where z is the distance from the substrate^{1,5,6}) and lateral ordering becomes less impor-

tant, so the average local density $n(\vec{r})$ depends mainly on z . Local properties of successive layers eventually approach those of the bulk. Physically important surface parameters, such as the excess surface density (n_s is the bulk density)

$$n_s = \int_0^\infty dz [n(z) - n_b], \quad (1)$$

involve measurement of substrate perturbations of bulk properties, i.e., the properties of the surface phase^{7,8} as it coexists with the bulk. It is the purpose of this paper to study the types of surface phase diagrams to be expected of multilayer systems. We shall neglect the details of lateral ordering almost entirely.

It is convenient to separate the basic energy scales of the adatom-adatom and adatom-substrate interactions from their distance dependence. Thus,

$$[V(\vec{r})]_{\text{atom-atom}} = v [f(\vec{r})]_{\text{atom-atom}}$$

and

$$[U(z)]_{\text{atom-substrate}} = u [f(z)]_{\text{atom-substrate}}, \quad (2)$$

where $f_{\text{atom-atom}}$ and $f_{\text{atom-substrate}}$ carry the distance dependence, while v and u set the energy scale and will be taken *negative* for attractive interactions. At this level of description there are, thus, four important energy parameters in the problem: the potential strengths $|v|$ and $|u|$, the thermal energy $k_B T$, and the chemical potential μ (measured relative to its coexistence value μ_0), which sets the density of the bulk adatom gas. Taking $|v|$ to fix the energy scale, we may imagine plotting the (μ, T)

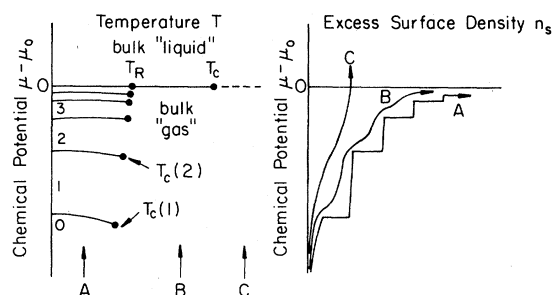


FIG. 1. Strong-substrate system, $u < u_w < 0$. Typical surface phase diagram with representative gas-phase adsorption isotherms. Surface phases are designated 0, 1, 2, 3, . . . , indicating the number of completed layers at $T=0$. Note the (infinite) sequence of layer transitions terminating in critical points $T_c(n)$, which approach the roughening temperature T_R , as $n \rightarrow \infty$. Isotherm *A* has an infinite number of sharp steps, while *B* and *C* are smooth. Isotherms *A* and *B* have $n_s \rightarrow \infty$ (complete wetting) as $\mu \rightarrow \mu_0^-$ (coexistence), while isotherm *C*, above coexistence, is smooth and finite.

phase diagram for different ratios $|u/v|$. It is our thesis that the form of the phase diagram is dependent crucially on this ratio and to a lesser but still important extent on the range of the adatom-adatom and adatom-substrate interactions. By varying these parameters we may study within the same context a wide range of physical phenomena, including layer formation, wetting, prewetting, and critical wetting. We shall consider interactions which are dominantly attractive, so $u, v < 0$.

It will facilitate discussion to present our conclusions here at the outset in qualitative form. Imagine that u is varied at fixed v , $f_{\text{atom-atom}}$, and $f_{\text{atom-substrate}}$. It turns out that there are three broad classes of systems: $|u| \gg |v|$ (i.e., $u \ll v < 0$), which we shall refer to as strong-substrate systems; $|u| \sim |v|$, which we shall call intermediate-substrate systems; and $|u| \ll |v|$ (i.e., $v \ll u < 0$), which we shall call weak-substrate systems. The boundaries between these regimes, u_w (between strong and intermediate) and u_c (between intermediate and weak), have a precise significance which we shall describe below and in Sec. II C. The intermediate and weak regimes are further subdivided, as we shall discuss below. Figures 1–5 show schematic phase diagrams and typical gas-phase adsorption isotherms for different ratios u/v . These sketches represent the case of short-ranged atom-atom attraction and longer-ranged atom-substrate attraction. They are illustrative only. As we shall see, other hybrid and limiting cases may occur. In particular, the range dependence is treated in Sec. III. Figure 6 depicts the full $(\mu, T, u/v)$ phase diagram for atom-atom and atom-substrate interactions which are of the nearest-neighbor type only.

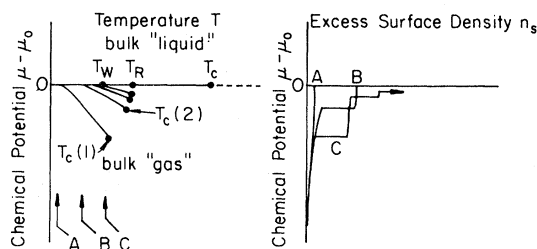


FIG. 2. Intermediate-substrate system in the layering subregion, $u_w < u < u_r < 0$. Typical surface phase diagram with representative gas-phase adsorption isotherms. At low temperatures there is little or no adsorption. As T is increased, the number of steps in the isotherms increases, becoming infinite at the wetting temperature T_w . For $T < T_w$, n_s remains finite (incomplete wetting) as $\mu \rightarrow \mu_0^-$. There is complete wetting at coexistence for $T_w < T < T_c$.

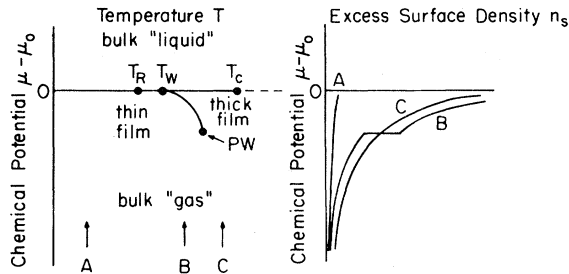


FIG. 3. Intermediate-substrate system in the prewetting subregion, $u_R < u < u_{CW} < 0$. Typical surface phase diagram with representative gas-phase adsorption isotherms. The point PW is the prewetting critical point. The prewetting line, joining T_W and PW, is a first-order phase boundary between thick- and thin-film behavior. For $T < T_W$, n_s remains finite as $\mu \rightarrow \mu_0^-$. For $T_W < T < T_C$ wetting at coexistence is complete.

The effect of long- versus short-ranged attraction is covered in Secs. II B, II C, and III.

When the substrate potential is strong (u/v large, Fig. 1), an infinite sequence of transitions occurs, corresponding to condensation of successive monolayers.⁵ The critical temperatures of these layer transitions approach for high-order multilayers a well-defined temperature T_R (the roughening temperature) which is less than the critical temperature T_c .⁹ At temperatures below T_R isotherms¹⁰ for the excess surface density n_s show an infinite sequence of sharp steps as $\mu \rightarrow \mu_0^-$ (bulk coexistence), corresponding to Dash's class-I behavior.¹¹ Between T_R and T_c the steps are rounded; however, n_s still diverges as $\mu \rightarrow \mu_0^-$. The divergence of n_s as $\mu \rightarrow \mu_0^-$ is called "complete wetting at coexistence"¹²⁻¹⁷ and reflects the formation of a "wetting layer" which becomes infinitely thick as coexistence is approached from the gas phase for all $T < T_c$. (Complete wetting is also associated with other coex-

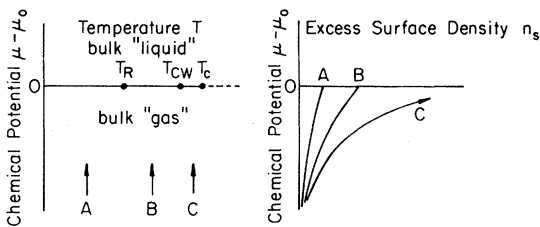


FIG. 4. Intermediate-substrate system in the critical wetting subregion, $u_{CW} < u < u_c < 0$. Typical surface phase diagram with representative gas-phase adsorption isotherms. The length of the prewetting line (Fig. 3) has shrunk to zero. Wetting at coexistence is incomplete below the critical wetting temperature T_{CW} and complete above.

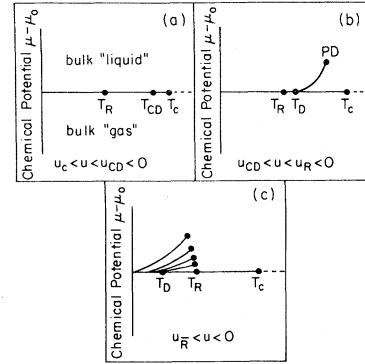


FIG. 5. Weak-substrate system, $u_c < u < 0$. Typical surface phase diagrams. (a) Critical drying subregion (no predrying); (b) predrying subregion, showing the predrying critical point PD and the predrying line; (c) layering subregion. The layering sequence now corresponds to stepwise buildup of less-dense layers as coexistence is approached from the high-density phase. Layer critical points terminate at T_R . The layering subregion occurs for the lattice-gas model (Sec. II) but not for real, continuum fluids (Sec. IV).

istence phenomena, as discussed in Sec. II C.) For $T > T_c$ there is no longer any bulk phase transition and $n_s(\mu)$ is smooth and finite at $\mu = \mu_0$.

As the strength of the substrate potential is de-

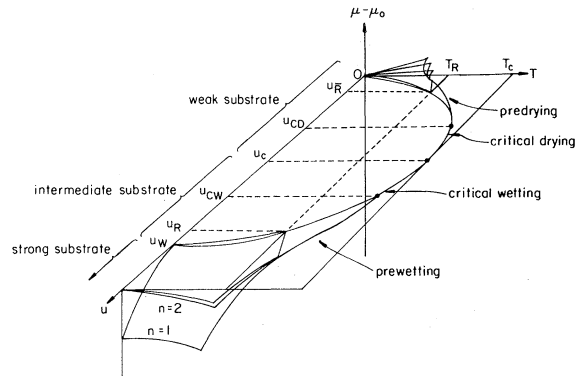


FIG. 6. Full T, μ, u surface phase diagram. The adatom-adatom potential is fixed. The overall strength u of the substrate potential becomes more attractive upon going away from the origin (left) along the u axis. The plane $\mu = \mu_0, T < T_c$ corresponds to bulk coexistence. Layering and predrying surfaces are below the coexistence plane (i.e., in the bulk-gas region) for $u < u_c$. Layering and predrying surfaces are above the coexistence plane (i.e., in the bulk-liquid region) for $u_c < u < 0$. This sketch corresponds to the case of $d = 3$ with nearest-neighbor-only interactions. Except for the slight differences between nearest-neighbor and long-range adatom-substrate potentials (see Sec. II C), Figs. 1-5 correspond to sections at fixed u through Fig. 6.

creased beyond u_W , one reaches the regime of intermediate substrates (Figs. 2–4). The layer transitions no longer extend¹⁸ to the $T=0$ axis but now meet the coexistence axis at and below a characteristic wetting temperature^{13–17} T_W ($0 < T_W < T_c$). For moderately strong substrate potentials ($u_W < u < u_R$) T_W remains below T_R (“layering” subregion of the intermediate-substrate regime) and the phase diagram (Fig. 2) is not very different from Fig. 1, except that the layer transitions now accumulate on the coexistence axis at T_W . Thus, at sufficiently low temperatures the isotherms show little or no observable excess surface density at any pressure short of coexistence (Dash’s “class¹⁹ III”). For $T \lesssim T_W$ there are a finite number of layer transitions as μ approaches μ_0 from below, $n_s(\mu = \mu_0^-)$ is finite (Dash’s class II), and the surface is “incompletely wet” at coexistence. (Other manifestations of incomplete wetting are discussed in Sec. II C.) Above T_W the surface is completely wet at coexistence and isotherms are similar to those of Fig. 1. If the substrate is weakened further ($u_R < u < u_{CW}$), T_W increases beyond²⁰ T_R (Fig. 3, “prewetting” subregion), high-order layer transitions cannot remain distinct, and the infinite sequence of layer transitions is replaced by a single thin-thick prewetting transition of the type discussed by Ebner and Saam⁶ and by Cahn.¹³ $n_s(\mu_0^-)$ is finite for $T < T_W$ (incomplete wetting) and infinite for $T_W < T < T_c$ (complete wetting). Isotherms are smooth, unless they cross the prewetting phase boundary, in which case they undergo a finite jump. Below T_W they are class II; above, class I. For still weaker substrates ($u_{CW} < u < u_c$), the prewetting line probably reduces²¹ to a single “critical-wetting” point on the coexistence curve (Fig. 4, critical-wetting subregion). Here, isotherms are smooth at *all* temperatures but switch from class II to class I at T_W .

Finally, for $u = u_c < 0$, T_W reaches T_c . Beyond this (i.e., for $u_c < u < 0$) is the regime of weak-substrate systems (Fig. 5). For such systems gas-phase behavior exhibits no anomalies¹⁸ and all isotherms are class II. What happens, however, is that the singular behavior shifts to the liquid side of the coexistence curve. There is a “drying temperature” T_D , above which $n_s \rightarrow -\infty$ as $\mu \rightarrow \mu_0^+$ (“complete drying,” class-I liquid-phase isotherms) and below which n_s is finite as coexistence is approached from the liquid phase (“incomplete drying,” class-II isotherms). As $|u|$ decreases from $|u_c|$ towards zero, the subregions identified for intermediate substrates are encountered in reverse order on the liquid-phase side of coexistence: critical drying,

predrying, layering.⁹ Since experiments have concentrated on the gas-phase side of coexistence, we shall not dwell further on the weak-substrate regime.

The physics behind this picture is as follows. A strong substrate potential u orders the layering systematically and reduces the adatom-adatom interaction to the role of controlling the in-layer condensation. As u decreases, it begins to have to compete with the forces which hold the liquid together (i.e., the forces responsible for the gas-liquid interfacial tension) and prefer droplet formation on the substrate to uniform wetting. This raises the wetting temperature T_W to a nonzero value, initiating the intermediate-substrate regime. Here, the low-temperature ($T < T_W$) behavior is dominated by energy considerations and favors class-II isotherms (incomplete wetting), while at higher temperatures ($T > T_W$) entropy contributions decrease the surface tension,¹³ so the substrate potential is more effective and isotherms change to class I (complete wetting). Whether thick-film growth takes place discretely, layer by layer, or all at once depends on the relative values of T_W and T_R . Finally, for $|u| < |u_c|$ interfacial-tension effects are strong enough to prevent complete wetting for all $T < T_c$ and anomalies shift to the liquid side of the coexistence curve.¹⁸ Behavior on the liquid side of the coexistence curve²² for $u = u_c + \Delta u$ is analogous to behavior on the gas side at $u = u_c - \Delta u$ by virtue of a “magnetic” symmetry described in Sec. II A.

The elements of which this systematics is composed certainly occur in the literature; however, so far as we are aware, they have not, except in special cases^{23–25} been integrated into a coherent picture, including the possibility of discrete layering and encompassing the strong-, intermediate-, and weak-substrate regimes. With the exception of Sullivan’s²³ work the central role of the ratio u/v does not seem to have been emphasized. The existence^{26–29} of systems (Figs. 2–4) with class-II (or even “class-III”) isotherms at low temperatures but class I at higher temperatures has not received sufficient theoretical attention. The available discussions of layering versus prewetting and critical wetting and the relation of these phenomena to coexistence behavior are fragmentary.

Our understanding is based in large part on the detailed analysis of a simple lattice-gas model of adsorption, originally introduced by de Oliveira and Griffiths.⁵ In Sec. II we introduce this model and discuss its properties both at $T=0$, where an exact analysis of ground-state energies and layering can

be carried out, and at coexistence ($\mu = \mu_0$), where the thermodynamics of wetting and roughening can be explored. Section III treats the full (T, μ) surface phase diagram. We have performed detailed mean-field calculations for interactions (both adatom-adatom and adatom-substrate) which are nearest-neighbor only. We discuss in the light of other theoretical work the probable effects of further-neighbor forces and of thermal fluctuations, neglected in the mean-field theory. Both of these extensions make significant and physically important changes in the mean-field phase diagram. Section IV examines the shortcomings of the lattice model itself, as a description of experiment, and attempts to identify those features which it may be expected to describe reliably and those which it may not. We conclude with a short discussion of the present experimental situation, which seems to lend some support to our picture, and some suggestions for future directions. Appendix A contains some results associated with the $T=0$ problem. Appendix B discusses adsorption in two (bulk) dimensions, where one-dimensional layers adsorb on a one-dimensional substrate. A short summary of some of our results appears elsewhere.³⁰

We emphasize that the picture presented here describes what happens only in the strict static thermodynamic limit (see Sec. II). In experiments, particularly at low temperatures, long-lived metastable states may dominate what is seen. Furthermore, finite-size and radius-of-curvature effects have observable consequences (such as capillary condensation). Substrate inhomogeneity and impurity effects, ignored in our discussion, may also be important.¹

II. LATTICE-GAS MODEL OF ADSORPTION

A. The Hamiltonian

Following de Oliveira and Griffiths,⁵ we consider a gas of atoms adsorbed on a semi-infinite set of discrete lattice sites (Fig. 7 with $D, L \rightarrow \infty$) and described by occupation-number variables $n_i = 0, 1$, where the subscript i labels sites. We assume that the substrate may be represented by a single-particle potential acting on the adatoms.³¹ The adatoms interact with one another via pairwise forces. The combination which enters the grand canonical partition function is

$$\mathcal{H} - \mu N = \sum_{\langle i, j \rangle} v_{ij} n_i n_j + \sum_i (u_i - \mu) n_i, \quad (3)$$

where $\langle i, j \rangle$ denotes a sum over distinct pairs. For simplicity we take the lattice to be hypercubical. Note that in this form the adatom kinetic energy contribution has been suppressed. In a *classical* treatment inclusion of the kinetic energy produces a temperature-dependent difference between the physical chemical potential μ_{phys} and the lattice-gas chemical potential appearing in (3),

$$\mu = \mu_{\text{phys}} + Td \ln(a/\Lambda), \quad (4)$$

where d is the dimensionality, a is the lattice spacing, and $\Lambda = (\hbar^2/2\pi m k_B T)^{1/2}$ is the thermal wavelength. This does not affect the difference $\mu_{\text{phys}} - (\mu_0)_{\text{phys}} = \mu - \mu_0$ plotted in Figs. 1–6.

We shall assume that the single-particle potential u_i is translationally uniform in directions parallel to the substrate surface,

$$u_i = u_n \quad \text{for } i \text{ in the } n\text{th layer}. \quad (5)$$

Typically u_n is attractive ($u_n \leq 0$) and falls off away from the substrate as^{1,6} n^{-3} . Reference 5 uses the parametrization (for $d=3$)

$$u_n = -A\delta_{n1} - Bn^{-3}. \quad (6)$$

The adatom-adatom interaction is assumed invariant under translations and point-group symmetries of the (bulk) lattice. It will be convenient in what follows to define layerwise sums over the pair interactions,

$$v_n \equiv \sum_j v_{ij} \quad (7)$$

for i in layer m and j in layer $m+n$ ($v_n = v_{-n}$). We shall discuss at length in Sec. III a model for which all interactions are of the nearest-neighbor type only,

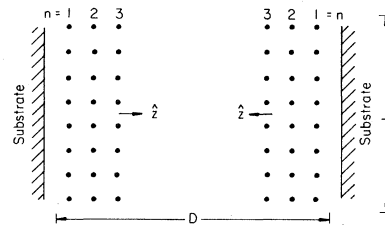


FIG. 7. Lattice structure for the model (3). There are D layers with L^{d-1} sites per layer. The direction perpendicular to the substrate is \hat{z} . The layers are taken to be periodically connected in directions perpendicular to \hat{z} . In the thermodynamic limits (16) and (17) both L and D go to infinity. Note that the “slab” is bounded by substrate on both sides.

$$u_n = u\delta_{n1}$$

and

$$v_{ij} = \begin{cases} v, & ij \text{ nearest neighbors} \\ 0 & \text{otherwise,} \end{cases} \quad (8a)$$

so

$$v_n = \begin{cases} 2(d-1)v, & n=0 \\ v, & n=1 \\ 0, & n>1. \end{cases} \quad (8b)$$

The model (3) is equivalent to a spatially inhomogeneous spin- $\frac{1}{2}$ Ising model

$$\begin{aligned} \mathcal{H}_{\text{Ising}} = \text{const} - \sum_i (H + H_i)\sigma_i \\ - \sum_{\langle ij \rangle} J_{ij}\sigma_i\sigma_j, \quad \sigma_i = \pm 1 \end{aligned} \quad (9)$$

provided that

$$\begin{aligned} \sigma_i &= 2n_i - 1, \\ H &= \frac{1}{2} \left[\mu - \frac{1}{2} \sum_j v_{ij} \right], \\ H_i &= \frac{1}{2} \left[-u_i + \frac{1}{2} \sum_j' v_{ij} \right], \\ J_{ij} &= -\frac{1}{4} v_{ij}, \end{aligned} \quad (10)$$

where the prime on the summation indicates that only "virtual" sites j , lying in the region occupied by the substrate, are to be counted. Because the bulk magnetic transition takes place at $H=0$, the lattice-gas coexistence curve is at

$$\mu_0 = \frac{1}{2} \sum_j v_{ij} = \frac{1}{2} v_0 + \sum_{m=1}^{\infty} v_m, \quad (11)$$

which reduces for $d=3$ and nearest-neighbor interactions (8) to

$$\mu_0 = 3v. \quad (12)$$

The usual magnetic symmetry, $\sigma_i \leftrightarrow -\sigma_i$, $H \leftrightarrow -H$, $H_i \leftrightarrow -H_i$, $J_{ij} \leftrightarrow J_{ij}$, corresponds to a lattice-gas symmetry,

$$\begin{aligned} n_i &= 0 \leftrightarrow n_i = 1, \\ \mu - \mu_0 &\leftrightarrow \mu_0 - \mu, \\ -u_i + \frac{1}{2} \sum_j' v_{ij} &\leftrightarrow u_i - \frac{1}{2} \sum_j' v_{ij}, \\ v_{ij} &\leftrightarrow v_{ij}. \end{aligned} \quad (13)$$

Thus, any phenomena occurring in the gas phase at $\mu = \mu_0 - \Delta\mu$ for a substrate potential

$$u_n = \frac{1}{2} \sum_{m=n}^{\infty} v_m + \Delta u_n \quad (14a)$$

will have an image $\mu' = \mu_0 + \Delta\mu$ in the liquid phase for the (different) substrate potential

$$u_n' = \frac{1}{2} \sum_{m=n}^{\infty} v_m - \Delta u_n. \quad (14b)$$

For interactions which are of the nearest-neighbor type only [Eq. 8(a)], this gives the whole phase diagram (e.g., Fig. 6) reflection symmetry in the line $u = u_c = \frac{1}{2}v$, $\mu = \mu_0$. For non-nearest-neighbor interactions, this symmetry of the *phase diagram* is not exact; however, a qualitative correspondence between gas-phase behavior at $u = u_c + \Delta u$ and liquid-phase behavior at $u = u_c - \Delta u$ is retained.

To discuss the thermodynamics, it will be convenient to consider a rectangular slab (Fig. 7) containing DL^{d-1} sites, arranged in D layers of L^{d-1} sites each. The slab is bounded on two opposite sides by substrate. It is connected periodically in the transverse directions and has free energy

$$F_{L,D}(T, \mu) = -k_B T \ln \text{Tr} e^{-\beta(\mathcal{H} - \mu N)}. \quad (15)$$

The bulk free energy per lattice site (i.e., the free energy per unit volume measured in unit cells) is defined by the thermodynamic limit,³²

$$f_b(T, \mu) = \lim_{L,D \rightarrow \infty} F_{L,D}(T, \mu) / DL^{d-1}, \quad (16)$$

which depends on the pair interactions $\{v_{ij}\}$. Similarly, the surface free energy per unit area is (remember, the slab has *two* faces)

$$\begin{aligned} f_s(T, \mu) = \lim_{L,D \rightarrow \infty} [F_{L,D}(T, \mu) \\ - DL^{d-1} f_b(T, \mu)] / 2L^{d-1}, \end{aligned} \quad (17)$$

which depends on both $\{v_{ij}\}$ and $\{u_n\}$ and assumes $\mu \neq \mu_0$ (single-phase bulk). Under suitable conditions this limit has been proved⁷ to exist, with f_s bounded and convex as a function of surface (but not bulk) potentials. It follows, for example, that f_s is necessarily continuous across surface phase boundaries (but may be discontinuous across bulk transitions, as at coexistence).

In addition, we shall need in our discussion of wetting the interfacial free energy. If the sample is

at “liquid-gas”³³ coexistence ($\mu = \mu_0$, $T < T_c$) and so arranged³⁴ as to contain a planar interface between the two phases of area A (measured in surface unit cells), oriented perpendicular to the unit vector \hat{n} ,

$$f_i(T, \hat{n}) = \lim_{L, D \rightarrow \infty} \{F_{L, D} - DL^{d-1}f_b - 2L^{d-1}[\alpha f_s(\mu = \mu_0^-) + \beta f_s(\mu = \mu_0^+)]\} / A, \quad (18)$$

which depends on \hat{n} , T , and $\{v_{ij}\}$ but not $\{u_n\}$. The coefficients α and β ($\alpha + \beta = 1$) specify the fractions of the slab faces in contact with the two bulk phases. The \hat{n} dependence is a consequence of the lattice structure of the model.³³

B. Analysis at $T = 0$

The $T = 0$ analysis is instructive in that it can be carried out exactly; however, the technical details are not crucial to what follows and may be skipped by the more casual reader. The ground state of Eq. (3) gives the structure of the system at $T = 0$. For sufficiently general interactions $\{u_n\}$ and $\{v_n\}$ the structure can be very complicated. We shall make the simplifying assumptions that $\{u_n\}$ and $\{v_n\}$ are both attractive (nonpositive) and that $\{u_n\}$ decays

then the corresponding additional contribution to the free energy $F_{L, D}$ defines an interfacial free energy per unit area (the interfacial or “surface” tension),

monotonically with distance. These assumptions cover many physical situations³⁵ and are sufficient to eliminate extraneous symmetry breaking, such as the formation of “antiferromagnetic” or otherwise structured phases, either bulk or surface. [Such effects are important in connection with epitaxial and incommensurate ordering (see Sec. IV) but would add an unrewarding complication here.] Under these conditions the bulk “gas” consists entirely of empty sites and the bulk “liquid,” of full sites. Furthermore, in the slab geometry and for $\mu > \mu_0$ (liquid phase l) the ground state of (3) has all layers full, while for $\mu < \mu_0$ (gas phase g) the relevant states can all be labeled by the number $n = 0, 1, 2, \dots$ of completed layers lying next to the substrate. The corresponding energies $E(\mu) = (\mathcal{H} - \mu N) / L^{d-1}$ per column of Fig. 7 are

$$E_n^{(g)}(\mu) = \begin{cases} 0, & n = 0 \\ 2 \left[\sum_{m=1}^n u_m + \frac{n}{2} v_0 + (n-1)v_1 + (n-2)v_2 + \dots + v_{n-1} - \mu n \right], & 0 < n < D/2 \end{cases} \quad (19a)$$

$$E^{(l)}(\mu) = 2 \sum_{m=1}^{\infty} u_m + \frac{D}{2} v_0 + (D-1)v_1 + (D-2)v_2 + \dots - D\mu, \quad (19b)$$

where we have taken D large compared to the range of both u_n and v_n . In the thermodynamic limit (16) gives

$$f_b(T=0, \mu) = \begin{cases} 0, & \mu < \mu_0 \\ \mu_0 - \mu, & \mu > \mu_0 \end{cases} \quad (20)$$

and it follows from (17) that

$$f_s(T=0, \mu) = \begin{cases} \min_n \left[\frac{1}{2} E_n^{(g)}(\mu) \right], & \mu < \mu_0 \\ \sum_{n=1}^{\infty} \left(u_n - \frac{1}{2} n v_n \right), & \mu > \mu_0. \end{cases} \quad (21a)$$

$$\sum_{n=1}^{\infty} \left(u_n - \frac{1}{2} n v_n \right), \quad \mu > \mu_0. \quad (21b)$$

A calculation similar to the above gives the interfacial free energy per unit area for an interface parallel to the substrate surface,

$$f_I(T=0, \hat{z}) = -\frac{1}{2} \sum_{n=1}^{\infty} n v_n. \quad (22)$$

Two important inequalities follow directly from the above expressions. Because interactions were assumed attractive ($v_n \leq 0$), Eq. (22) shows

$$f_I(T=0, \hat{z}) > 0. \quad (23)$$

Furthermore, direct evaluation of (21) gives

$$\begin{aligned} -f_I(T=0, \hat{z}) &\leq f_s(T=0, \mu_0^-) - f_s(T=0, \mu_0^+) \\ &\leq f_I(T=0, \hat{z}). \end{aligned} \quad (24)$$

Simple physical arguments show that both these inequalities are, in fact, quite general, extending to

interactions which are neither purely attractive nor monotonic (and, indeed, to $T > 0$, as we shall see in Sec. II C). The postivity (23) of the interfacial free energy at $T = 0$ guarantees that near $\mu = \mu_0$ the system is energetically stable against the creation of opposite-phase inclusions in the bulk. Similarly, Eq. (24) expresses a bound on the free-energy discontinuity at μ_0 , based on a perturbation in which the whole bulk region, away from the walls, changes phase: Denote by superscripts l and g configurations which are, respectively, liquidlike and gaslike far from the walls. Any gaslike configuration can be made liquidlike (and conversely) by taking an entire interior region of layers, far from both boundaries, and reversing all site occupations $0 \leftrightarrow 1$. This creates two interfaces and costs an energy per column $2f_1(T=0, \hat{z})$. Application of this procedure to the minimum-energy gaslike state creates a liquidlike state with energy

$$\begin{aligned} E^{(l)}(\mu_0) &= \min E^{(g)}(\mu_0) + 2f_1(T=0, \hat{z}) \\ &\geq \min E^{(l)}(\mu_0). \end{aligned} \quad (25)$$

Because bulk free energies per unit volume are equal at coexistence,

$$\begin{aligned} f_s(T=0, \mu_0^-) - f_s(T=0, \mu_0^+) \\ = \frac{1}{2} [\min E^{(g)}(\mu_0) - \min E^{(l)}(\mu_0)], \end{aligned} \quad (26)$$

so Eq. (25) gives the left-hand half of Eq. (24). The other half follows similarly, starting from the minimum-energy liquidlike state.

The $T = 0$ results (19)–(22) provide insight into two important questions. (i) When is there an infinite sequence of layer transitions (Fig. 1, Dash's class I) and when, on the other hand, does the system jump directly from a finite surface-density enhancement to bulk-liquid behavior (Figs. 2–5, Dash's classes II and III)? (ii) If layers form, what determines their sequencing? Question (i) will turn out to be directly related to the existence of a wetting transition. To establish the existence and sequencing of layering for $\mu < \mu_0$ requires carrying out the minimization in (21a). Details depend on the specific forms of $\{u_n\}$ and $\{v_n\}$; however, a few more general statements can be made:

(a) Because of the form of Eqs. (19a) and (21a), $f_s(T=0, \mu)$ is convex upward³⁶ for all $\mu < \mu_0$ (see also Appendix A). Furthermore, the linear μ dependence guarantees that the $n = 0$ state is preferred for all sufficiently negative μ .

(b) If the n th-layer transition ($n - 1$ layers goes to n layers) occurs, it takes place at a chemical potential μ_n defined by $E_{n-1}^{(g)}(\mu_n) = E_n^{(g)}(\mu_n)$, which gives

$$\mu_n = \mu_0 + u_n - \sum_{m=n}^{\infty} v_m. \quad (27)$$

(c) A necessary but not sufficient condition for occurrence of the n th-layer transition is $\mu_0 - \mu_n > 0$. If the substrate potential is regarded as composed of contributions w_m from successive substrate layers,

$$u_n = \sum_{m=n}^{\infty} w_m \quad \text{with } w_m \equiv u_m - u_{m+1}, \quad (28)$$

then this condition takes the form

$$\sum_{m=n}^{\infty} (v_m - w_m) > 0, \quad (29)$$

which has the interpretation that the tail beyond layer n of the substrate potential must be more strongly attractive than the corresponding tail of the particle-particle potential. Note that w_n is negative if $\{u_n\}$ is attractive and monotone decreasing in magnitude.

(d) We call the transitions "locally sequential" if $\mu_{n+1} \geq \mu_n$. This is equivalent via (27) to

$$u_{n+1} - u_n + v_n = v_n - w_n \geq 0 \quad (30)$$

and means that the attraction of the n th substrate layer dominates that of the corresponding adatom layer. Equation (30) does not, of course, guarantee that the n th- and $(n + 1)$ st-layer transitions actually occur—only that they may occur sequentially, provided that other layer configurations do not have lower energy. Equality in (30) means that the allowed range in μ of the n -layer phase has shrunk to zero, a situation which develops, for example, when both $\{u_n\}$ and $\{v_n\}$ are of strictly finite range.

(e) A necessary and sufficient condition that an infinitely thick "wetting film" should build up as $\mu \rightarrow \mu_0^-$ (as, e.g., in Fig. 1) is that $E_n^{(g)}(\mu_0) > E_{\infty}^{(g)}(\mu_0)$ for all $n < \infty$. The necessity of this condition follows from continuity; sufficiency uses in addition the convexity property (a). Direct evaluation of this condition gives³⁷

$$\begin{aligned} \frac{1}{2} [E_n^{(g)}(\mu_0) - E_{\infty}^{(g)}(\mu_0)] \\ = - \sum_{m=n+1}^{\infty} [u_m - (m-n)v_m] > 0. \end{aligned} \quad (31)$$

(f) A sufficient but not necessary condition for wetting is that the n -layer phase occur and that Eq. (30) [and thereby Eq. (29)] hold for all $m > n$.

(g) If wetting occurs, then³⁷

$$\begin{aligned} f_s(T=0, \mu_0^-) &= \frac{1}{2} E_{\infty}^{(g)}(\mu_0) = \sum_{n=1}^{\infty} (u_n - n v_n) \\ &= f_s(T=0, \mu_0^+) + f_1(T=0, \hat{z}), \end{aligned}$$

so the right-hand side of Eq. (24) holds as an equality. Furthermore, for large n (where v_n and u_n vary smoothly with n) the minimization condition $\partial E_n^{(g)}/\partial n=0$ reproduces Eq. (27), which then determines the thickness $t(\mu)$ of the wetting film for $\mu \lesssim \mu_0$.

(h) When the substrate potential vanishes, then $n=0$ minimizes Eq. (21a); so $f_s(T=0, \mu_0^-)=0$ and

$$\lim_{n \rightarrow \infty} (u_n/nv_n) \text{ and } \lim_{n \rightarrow \infty} (w_n/v_n) = \begin{cases} \infty, & \text{if } \{u_n\} \text{ "dominates"} \\ \text{positive constant,} & \text{if } \{u_n\} \text{ and } \{v_n\} \text{ are "comparable"} \\ 0, & \text{if } \{v_n\} \text{ "dominates."} \end{cases} \quad (32)$$

Now, consider an attractive substrate potential $u_n \equiv u f_n$ of fixed shape but with an overall strength u which is variable, as in Eq. (2). When the long-range behavior of $\{u_n\}$ dominates or is comparable to that of $\{v_n\}$ (as, for example, when $\{v_n\}$ has strictly finite range), then at large enough $|u|$ Eq. (31) holds, wetting occurs as $\mu \rightarrow \mu_0^-$, and the thickness $t(\mu)$ of the wetting film is determined via (g) from Eq. (27). For example, if $u_n = -B/n^\theta$ as in Eq. (6), then³⁸

$$t(\mu) = [B/(\mu_0 - \mu)]^{1/\theta}, \text{ as } \mu \rightarrow \mu_0^-. \quad (33)$$

As $|u|$ is decreased, the minimum of Eq. (21a) switches to $n < \infty$ at a special value of the coupling u , which we denote u_W . For $u < u_W$ complete wetting occurs as $\mu \rightarrow \mu_0^-$ and $T=0$ behavior is class I; for $u_W < u < 0$ complete wetting does not occur and $T=0$ behavior is class II. On the other hand, if $\{v_n\}$ dominates at long distances (e.g., if $\{u_n\}$ is of strictly finite range and $\{v_n\}$ is not), then however large $|u|$ is the condition (31) fails for sufficiently large n , so complete wetting never occurs at $T=0$. These conclusions are relevant to our discussion of the wetting transition in Sec. II C.

Appendix A gives some detailed results for layer sequencing when the substrate interactions are attractive and monotonically decaying with distance and the particle-particle interactions are attractive and short ranged. When v_{ij} is nonvanishing between nearest neighbors only [Eq. 8(b)], then as μ increases to μ_0 the layering sequence can be (a) $[0, 1, 2, 3, \dots, \infty, \text{liquid}]$, (b) $[0, n, n+1, \dots, \infty, \text{liquid}]$ with $n > 1$, or (c) $[0, \text{liquid}]$. In cases (a) and (b) Eq. (31) is satisfied and a wetting film forms; in case (c) the surface remains incompletely wet right up to coexistence. Case (a) obtains when $|v| < |u_1 - u_2|$ (i.e., when the first two layers are strongly distinguished from one another on the

the left-hand side of Eq. (24) holds as an equality. For any attractive substrate potential the left-hand side of Eq. (24) holds as a strict inequality.

These results allow a systematic discussion of wetting at $T=0$. In this discussion the long-range behavior of $\{u_n\}$ and $\{v_n\}$ plays a crucial role. We define

scale of $|v|$), while (b) obtains when $|v| > |u_1 - u_2|$ (i.e., when they are not). It is easy to verify that u_W occurs when $v = \sum_{n=1}^{\infty} u_n$. When v_{ij} contains interactions between both first- and second-neighbor layers, then the additional layering sequences $[0, 1, n, n+1, \dots, \infty, \text{liquid}]$ and $[0, 1, \text{liquid}]$ can also appear for appropriate interaction parameters. The sequence $[0, 1, \text{liquid}]$ exhibits Dash's class-II behavior at $T=0$ and corresponds to failure of (31) (i.e., relatively weak substrate) with $|v_1| < |u_1 - u_2|$ (weak nearest-neighbor layer attraction v_1) and $|v_2| > \sum_{n=2}^{\infty} |u_n|$ (second-neighbor layer attraction dominates substrate tail). Additional possibilities occur for even longer-range particle-particle attractions. In Sec. III we shall explore the connection between $T=0$ behavior and the form of the full (T, μ) phase diagram.

C. Behavior near coexistence: Wetting, drying, and roughening

In this section we explore behavior near $\mu = \mu_0$. At $T > 0$ exact calculations cannot be done except in very special cases³⁹; however, a more or less complete picture emerges from qualitative considerations.

Connection with the usual surface and interfacial coefficients, which are only defined at coexistence, is established by^{40,41}

$$\gamma_{gs}(T) \equiv f_s(T, \mu \rightarrow \mu_0^-(T)), \quad (34a)$$

$$\gamma_{ls}(T) \equiv f_s(T, \mu \rightarrow \mu_0^+(T)), \quad (34b)$$

and

$$\gamma_{gl}(T, \hat{n}) \equiv f_1(T, \hat{n}). \quad (34c)$$

Note that (34a) and (34b) differ slightly from the

usual definitions in that they do not include the substrate-vacuum surface energy,¹ often denoted γ_{s0} , which is simply an additive constant for the inert substrate of our model. These coefficients satisfy two important inequalities,

$$\gamma_{gl}(T, \hat{n}) > 0 \quad (35)$$

and

$$-\gamma_{gl}(T, \hat{z}) \leq \gamma_{gs}(T) - \gamma_{ls}(T) \leq \gamma_{gl}(T, \hat{z}), \quad (36)$$

whose $T=0$ versions have already appeared as Eqs. (23) and (24). The positivity (35) of the interfacial tension is well known and follows from stability against macroscopic phase separation; however, we are aware of no rigorous proof. The right-hand-side inequality of (36) appears in the adsorption literature; however, to the best of our knowledge the left-hand side one does not⁴² (indeed, there have been suggestions that class-III behavior might be connected with its violation⁴³). Rigorous proof is again absent; however, generalization of the $T=0$ argument given after Eq. (24) appears possible.⁴⁴

In the absence of lateral symmetry breaking, the thermal-average density $n(z) \equiv \langle n_i \rangle$ for i in layer z , is uniform in directions parallel to the substrate and the excess surface density for the lattice model is [cf. Eq. (1)]

$$n_s(T, \mu) \equiv \sum_{z=1}^{\infty} [n(z) - n_b] = - \frac{\partial f_s(T, \mu)}{\partial \mu}, \quad (37)$$

where the last equality follows from (17). n_s may be either positive or negative. Away from phase boundaries it is finite and varies smoothly as a function of T and μ . We shall see below that the behavior of n_s as $\mu \rightarrow \mu_0$ is related to the occurrence of equalities in (36) and to crystallite formation on the substrate at coexistence.

1. Wetting and drying, complete and incomplete

When $n_s(T, \mu) \rightarrow \infty$ as $\mu \rightarrow \mu_0^-$ (e.g., a gas-phase isotherm), we shall refer to the substrate surface as⁴⁵ completely wet at coexistence (Dash's class I). When⁴⁶ $-\infty < n_s(T, \mu_0^-) < \infty$, the surface is⁴⁵ incompletely wet at coexistence (Dash's class¹⁹ II). The remaining alternative, $n_s(T, \mu) \rightarrow -\infty$ as $\mu \rightarrow \mu_0^-$, does not occur.⁴⁷ When $n_s(T, \mu) \rightarrow -\infty$ as $\mu \rightarrow \mu_0^+$ on the liquid side of coexistence we shall

call it complete drying (class \bar{I}), while $-\infty < n_s(T, \mu_0^+) < \infty$ is incomplete drying (class \bar{II}), and the final alternative, $n_s(T, \mu) \rightarrow \infty$ as $\mu \rightarrow \mu_0^+$, does not occur.⁴⁷

Consider first what happens when complete wetting occurs. Because $n(z) \leq 1$, the fact that $n_s \rightarrow \infty$ implies that the thickness $t(T, \mu)$ of the region of enhanced density must diverge as $\mu \rightarrow \mu_0^-$ (Fig. 8). When t is much larger than both the bulk correlation length ξ and the range r_0 over which the substrate potential is appreciable, then arguments of locality suggest that the density becomes more or less independent of z , $n(z) \simeq n_e$, over most of the film thickness t . As $\mu \rightarrow \mu_0^-$, n_b approaches the coexistence value of the bulk-gas density ($n_b^{(g)}$), n_e is expected to approach the coexisting bulk-liquid density ($n_b^{(l)}$), and n_s diverges as $(n_b^{(l)} - n_b^{(g)})t(T, \mu)$. At coexistence the bulk gas and bulk liquid have the same free energy per unit volume, so the only contributions to $\gamma_{gs}(T)$ come from the two widely separated nonuniform regions d_1 and d_2 in Fig. 8. It follows from this picture that^{48,49}

$$\gamma_{gs}(T) = \gamma_{ls}(T) + \gamma_{gl}(T, \hat{z}). \quad (38)$$

This relation, called Antonov's rule,^{42,50} is the thermodynamic counterpart of complete wetting and means that the right-hand side of (36) holds as an equality. Physically, complete wetting corresponds to the intrusion at coexistence of a layer of (bulk) liquid between the bulk gas and the substrate.⁴² For $\mu < \mu_0$ the gas-liquid interface may be regarded as "bound" to the substrate. When complete wetting occurs, the interface unbinds from the substrate continuously as $\mu \rightarrow \mu_0^-$. When there is incomplete

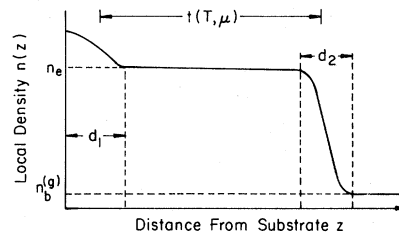


FIG. 8. Density profile, $n(z)$ as function of distance z above the substrate, under conditions such that complete wetting occurs at coexistence. $\mu \lesssim \mu_0$ (gas phase). The region of nonuniform behavior near the substrate has a width d_1 comparable to the larger of ξ (the bulk correlation length) and r_0 [the range over which $u(z)$ differs appreciably from zero]. The region of nonuniformity at the "interface" has a width $d_2 \sim \xi$. $n_b^{(g)}$ is the bulk-gas density. When $t \gg d_1, d_2$, the density n_e of the enhanced region is (nearly) uniform. As $\mu \rightarrow \mu_0^-$, $t \rightarrow \infty$ and n_e approaches the coexisting bulk-liquid density $n_b^{(l)}$.

wetting, the interface remains bound as $\mu \rightarrow \mu_0^-$.

The counterpart of complete wetting on the liquid side of coexistence is complete drying, $n_s \rightarrow -\infty$. A precise parallel of the argument leading to (38) gives

$$\gamma_{ls}(T) = \gamma_{gs}(T) + \gamma_{gl}(T, \hat{z}), \quad (39)$$

i.e., the left-hand side of (36) holds as an equality, corresponding to a gas-layer intrusion at coexistence between the liquid and the substrate.

Complete wetting and complete drying, defined in the limits $\mu \rightarrow \mu_0^\pm$, have important implications for behavior at coexistence. If the dense phase were an isotropic liquid, thus making applicable the Young-Duprès condition,⁴¹

$$\gamma_{gs} - \gamma_{ls} = \gamma_{gl} \cos \theta,$$

then equality in (36) would make the contact angle θ equal to zero or π , thus preventing droplets from forming on the substrate at coexistence. The anisotropy introduced by the lattice replaces the Young-Duprès condition by the Wulff construction,⁵¹ with (when the bulk phase is gas) the quantity $\gamma_{ls} - \gamma_{gs}$ in place of the interfacial tension for the crystallite facet which contacts the substrate.⁵² When $\gamma_{gs} - \gamma_{ls} > 0$, as it is when (38) holds, this requires that the equilibrium crystallite shape be outside the plane through $(\gamma_{gs} - \gamma_{ls})\hat{z}$ but inside the usual Wulff construction (see Fig. 9). Equation (38) reduces this available volume to zero, so surface crystallites do not form at coexistence. On the other hand, when (39) holds, a crystallite can form but it is completely independent of the substrate (i.e., $\theta = \pi$). In the intermediate regime, where (36) holds as a strict inequality, both wetting and drying are incomplete and there is no direct connection between the free-energy discontinuity across coexistence and the interfacial tension. Under these conditions the Wulff construction produces a well-defined equilibrium shape (see Fig. 9) and crystallite growth can proceed at coexistence. The foregoing discussion has an exact parallel on the liquid side of coexistence: Small voids can form on the substrate when (36) holds as a strict inequality but are suppressed by (38) or (39).

A surface which is completely wet at coexistence is covered by a film whose thickness $t(T, \mu)$ diverges as $\mu \rightarrow \mu_0^-$. The form of this divergence can be guessed by an appropriate generalization of the argument leading to Eq. (33). We suppose that the free energy of a situation described by a density profile $n(z)$ may be approximated as [cf. Eq. (19a)]

$$F(T, \mu, n(z)) \approx \sum_{z=1}^{\infty} (u_z^{\text{eff}} - \mu)n(z) + \frac{1}{2} \sum_{z, z'} v_{z-z'}^{\text{eff}} n(z)n(z'), \quad (40)$$

which neglects the thermal-fluctuation (entropic) effects due to finite T except insofar as they give rise to modified, temperature-dependent effective potentials $u_n^{\text{eff}}(T, \mu)$ and $v_n^{\text{eff}}(T, \mu)$. Near coexistence a film of thickness t may be approximated by a profile⁵³

$$n(z) = \begin{cases} n_b^{(l)}, & z \leq t \\ n_b^{(g)}, & z > t \end{cases}$$

with $n_b^{(l)} + n_b^{(g)} = 1$. Minimization of (40) with respect to t gives⁵⁴ [cf. Eq. (27)]

$$\mu = \mu_0 + u_t^{\text{eff}} - \sum_{z=t}^{\infty} v_z^{\text{eff}}. \quad (41)$$

Solving for $t(T, \mu)$ provides the film thickness near coexistence, assuming that the effective potentials are known. Just as at $T=0$, complete wetting ($t \rightarrow \infty$ as $\mu \rightarrow \mu_0^-$) requires that the combination $u_t^{\text{eff}} - \sum_{z=t}^{\infty} v_z^{\text{eff}}$ be less than zero, i.e., that u_z^{eff} dominates v_z^{eff} for large z [in the sense of Eq. (32)]. No first-principles calculations of $t(T, \mu)$ or the effective potentials u^{eff} and v^{eff} are presently avail-

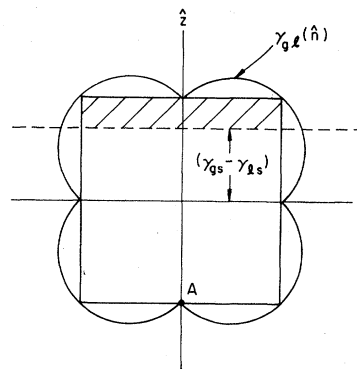


FIG. 9. Illustration of the Wulff construction for crystallite growth on a surface at coexistence (Ref. 52). The square represents the equilibrium crystal shape in the absence of the substrate. The allowed volume (cross-hatched) is within the square but outside a plane perpendicular to \hat{z} and through the point $(\gamma_{gs} - \gamma_{ls})\hat{z}$. When Eq. (38) holds (complete wetting), the allowed region shrinks to zero and no crystallite formation is possible. When Eq. (39) holds (complete drying), the plane passes through the point A and crystallites no longer use the substrate surface. As long as Eq. (36) holds as an inequality, the Wulff construction gives a well-defined surface-crystallite (surface—small-void) shape.

able; however, qualitative behavior can be inferred from (41). Away from criticality Ising-model correlations die off exponentially as $e^{-r/\xi}$, where $\xi(T, \mu)$ is the bulk coherence length. When $T < T_R$, it is hard to see how this kind of short-ranged effect can modify the form of a long-ranged potential such as Eq. (6). Thus, if v_n is not of longer range than u_n , we expect for (6) $u_n^{\text{eff}} = -B(T)/n^3$ so that, when complete wetting occurs,

$$t(T, \mu) \sim [B(T)/(\mu_0 - \mu)]^{1/3} \quad (42)$$

[cf. Eq. (33)] and layer transitions are spaced as $\mu_0 - \mu_n \sim B(T)/n^3$ [cf. Eq. (27)], where we have allowed the possibility of a temperature-dependent coefficient $B(T)$. On the other hand, if both u_n and v_n have strictly finite range as in Eq. (8a), then it seems reasonable to expect that the thermal fluctuations will produce an exponential tail $u_n^{\text{eff}} = -C(T)e^{-n/\xi}$ and similarly for v_n^{eff} . Thus, when complete wetting occurs (i.e., for u sufficiently attractive)

$$t(T, \mu) \sim \xi \ln[(\mu_0 - \mu)/C(T)],$$

with layer-transition spacing $\mu_0 - \mu_n = C(T)e^{-n/\xi}$. When $T > T_R$, interfacial roughening effects may produce long-range (i.e., power-law rather than $e^{-n/\xi}$) modifications of the bare potentials, so the above conclusions may be significantly modified.^{55(a)} We shall return to this point in the next subsection. Long-range *transverse* correlations associated with the approach to complete wetting have recently been discussed by several authors.^{55(b)}

Complete wetting (class-I isotherms) and incomplete wetting (class-II isotherms) have both been observed in a variety of adsorption experiments.^{11,23} Analogous observations have also been made on three-phase fluid-fluid-vapor systems.⁵⁶⁻⁵⁸ Complete drying, on the other hand, shows up in liquid-phase isotherms. It has only recently been discussed^{15,59} and has not to our knowledge been observed directly. It is tempting to guess that such extreme class-II (Dash's class III) situations as H_2O on graphite⁶⁰ and mercury on glass may correspond to complete drying on the liquid side of coexistence.

2. The wetting and drying transitions

Figure 10 is a sketch of the coexistence plane $\mu = \mu_0$ for $d=3$ in the rather special case of nearest-neighbor interactions (8). It is a consequence of the magnetic symmetry (14) that $T_W(u)$ and $T_D(u)$ and the associated regions of complete

and incomplete wetting and drying are exactly symmetrical about the line $u = v/2$ (corresponding in magnetic language to $H_i = 0$ for all sites i). The $T=0$ analysis of Sec. II B identifies $u_W = v$, so $T_W(v) = T_D(0) = 0$. The fact that $u_c = v/2$ (i.e., that at $u = v/2$ behavior is class II, $\bar{\text{II}}$ for *all* temperatures $T < T_c$) is equivalent to the statement in magnetic language that when $\{H_i = 0\}$ the excess surface magnetization remains finite as $H \rightarrow 0^\pm$ for all $T < T_c$. While to our knowledge not rigorously proven in $d=3$, this statement is, we believe, reliable: It respects the symmetry, is rigorous⁶¹ in $d=2$ (Appendix B), and certainly holds in mean-field theory (Sec. III A). Notice that a strong substrate potential favors complete wetting, while a weak one favors complete drying. At fixed u the competition between complete and incomplete wetting (drying) is between substrate forces, which favor orderly layering, and interfacial tension, which inhibits layering and favors crystallite (droplet) formation (class II or $\bar{\text{II}}$). Increasing T reduces the interfacial tension and thus promotes complete wetting (drying). The wetting line $T_W(u)$ has special significance only on the *gas* side of coexistence, where it signals the unbinding of the interface, as the film thickness t diverges. There is no qualitative⁶² change in behavior near $T_W(u)$ on the liquid side of coexistence. Similarly, $T_D(u)$ is significant

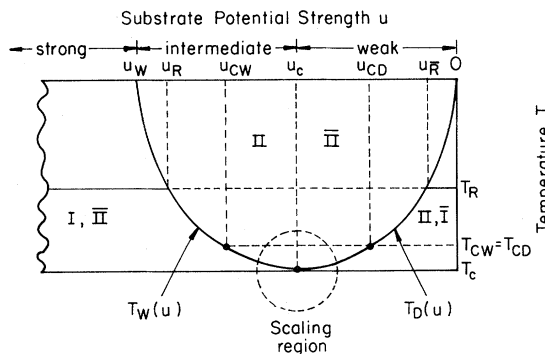


FIG. 10. Singularities at coexistence for $d=3$ (simple-cubic lattice) with nearest-neighbor interactions only. For this case $u_W = v$, $u_c = v/2$ (exact), and furthermore, $T_c \approx 1.128 |v|/k_B$, $T_R \approx 0.57T_c$. Reflection symmetry about the line $u = u_c$ takes the wetting curve $T_W(u)$ into the drying curve $T_D(u)$, etc. Roman numerals indicate the class of gas-phase (unbarred) and liquid-phase (barred) isotherms. Only under the wetting-drying curves (II, $\bar{\text{II}}$) can crystallites form at coexistence. The scaling described by (47)–(49) holds in the region near $u = u_c$, $T = T_c$. The curves along which layer transitions meet the coexistence plane are not shown in this figure.

for behavior only on the liquid side of coexistence and cannot be used to make a *sharp* distinction between Dash's class-II and class-III gas-phase isotherms.^{11,19} The form of the singular behavior near $T_W(u)$ as $\mu \rightarrow \mu_0^-$ and near $T_D(u)$ as $\mu \rightarrow \mu_0^+$ will be discussed below.

For interactions which are not nearest-neighbor only the coexistence phase diagram loses the exact symmetry of Fig. 10 but nevertheless retains its general shape. The $T=0$ analysis at the end of Sec. IIB shows that complete wetting occurs for sufficiently large $|u|$, provided only that u_n is not dominated by v_n at large n [in which case Eqs. (29) and (30) can never be satisfied at large n]. There is an interval $u_W(v) < u < 0$ in which incomplete wetting and drying occur at $T=0$. Furthermore, Antonov's relations (38) and (39) hold at $u=u_W$ and $u=0$, respectively [see comments (g) and (h) of Sec. IIB], so

$$T_W(u_W) = T_D(0) = 0. \quad (43)$$

The existence of a unique u_c with

$$T_W(u_c) = T_D(u_c) = T_c \quad (44)$$

is not rigorous but seems firm. It is certainly true in mean-field theory. Indeed, experience with magnetic surfaces⁶³ suggests that there is only one relevant surface-field variable, which we may take to be $\delta u \equiv u - u_c$. If this is so, then local changes in v_{ij} and u_i (such as further-neighbor interactions) may shift u_c but will not change its character. The upshot (Fig. 11) is a coexistence phase diagram which is broadly similar to Fig. 10 but possesses some features which are sensitive to the long-distance competition between u_n and v_n , as we now elaborate.

When u_n and v_n both have strictly finite range [Fig. 11(a)], then the coexistence phase diagram is simply a distorted version of Fig. 10. Notice in particular that when $u=0$ there is complete drying on the liquid side of coexistence for all $0 < T < T_c$. The physics of this is as follows. As long as t (the thickness, now, of the *drying* layer) is larger than the range of the atom-atom potential, the position of the interface is neutral (undetermined) at $T=0$; however, for any $T > 0$ the interface has thermal fluctuations, which are inhibited by the substrate surface, so there is an entropy effect which favors large over small t and causes the interface to unbind from the substrate. If v_n remains of strictly finite range but u_n becomes long ranged ($u_n \sim -B/n^\Theta$), then the coexistence phase diagram [Fig. 11(b)] is modified near $u=0$: Although drying is complete

at $u=0$ (where the problem is identical to the finite-ranged case), there is now incomplete drying arbitrarily close to $u=0$ at low temperatures. This discontinuous behavior is most easily understood by using the magnetic symmetry (14) to map to a corresponding wetting problem: Beyond the range of $v_n, u_n = \Delta u_n$, so $u'_n = -\Delta u_n = -u_n$. Thus, drying behavior with a weakly *attractive* substrate maps to wetting behavior with a weakly *repulsive* substrate (at long distances). This repulsion violates Eq. (29) [or, equivalently, the condition after (41) that $u'_t - \sum_{z=t}^{\infty} v'_z < 0$] and prevents complete wetting with $\{u'_n\}$ and, therefore, complete drying with $\{u_n\}$. As T increases, the weak attraction $\{u_n\}$ competes with the repulsion of the interface due to thermal fluctuations. Provided that $T < T_R$, it seems likely that the power law $u_n \sim n^{-\Theta}$ is not modified [cf. the discussion surrounding Eq. (42)], so drying remains incomplete for $u < 0$; however, when $T_R < T < T_c$, interfacial wandering is known to produce power-law correlations⁶⁴ and it is reasonable to suppose that the interfacial (entropic) repulsion develops power-law behavior $\sim n^{-\Theta'}$ with an exponent $\Theta'(T)$ which decreases as T increases.

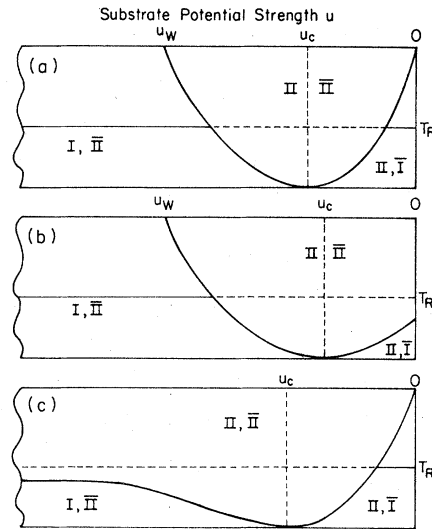


FIG. 11. Sketches of coexistence-plane phase diagrams for attractive potentials (a) $\{u_n\}$ and $\{v_n\}$ both of strictly finite range, (b) $\{u_n\}$ long range and $\{v_n\}$ of strictly finite range, (c) $\{u_n\}$ of strictly finite range and $\{v_n\}$ long range. Onsets u_{cw} and u_{cd} of critical wetting and drying are not shown. At $u=0$, $0 < T < T_c$ drying at coexistence is always complete (class I); however, in case (b) drying is incomplete (class II) for $u < 0$ at low temperatures. Similarly, in case (c) wetting remains incomplete at low temperatures even for very strong attraction u , as explained in the text.

As soon as $\Theta > \Theta'(T)$, complete drying occurs for small enough u . This behavior of the entropic repulsion is, of course, beyond mean-field calculations. It remains conjectural pending a realistic calculation. It is possible, for example, that for small enough Θ , $\Theta'(T)$ remains larger than Θ for all $T < T_c$, and so $u_c = 0$. Modification of Fig. 11(a) for the case of atom-atom attractions which are long-range ($v_n \sim n^{-\Theta}$) with atom-substrate attractions of strictly finite range is shown in Fig. 11(c) and also deserves comment. Here, u_n vanishes at large n , so Eq. (29) can never be satisfied at $T = 0$ even for very large $|u|$ ($u_W \rightarrow -\infty$). As T increases, the entropic repulsion (which may here be thought of as a repulsive contribution to u_n^{eff}) competes with v_n , so for large enough $|u|$ we expect crossover to complete wetting behavior at $T_R < T_W(u) < T_c$. A corresponding discussion of the situation when both $\{u_n\}$ and $\{v_n\}$ are long-ranged is certainly possible; however, it would require a better understanding of the thermally modified exponents $\Theta'(T)$ than we now possess. Suffice it to say that, when u_n and v_n are comparable in the sense of Eq. (32) (which applies, for example, to the physically interesting case when both arise from van der Waals interactions), then a coexistence phase diagram similar to Fig. 11(a) seems likely.

Near enough the bulk critical temperature ($T \leq T_c$) the substrate surface is always completely wet or completely dry at coexistence. An argument to this effect was first advanced by Cahn,¹³ who noted [$t \equiv |(T - T_c)/T_c|$]

$$\gamma_{gl} \sim t^\mu \quad (45)$$

and argued further that⁶⁵

$$\gamma_{gs} - \gamma_{ls} \sim u_1 [n_g(z=1) - n_l(z=1)] \sim t^{\beta_1}, \quad (46)$$

with⁶³ $\mu = (d-1)\nu = 2 - \alpha - \nu$ and $\beta_1 = (d-1)\nu - \Delta_s^{(0)}$. Here, ν , α , and $\Delta_s^{(0)}$ are the exponents associated with the bulk correlation length, the bulk specific heat, and the surface field, respectively. Incomplete wetting near T_c would require $\gamma_{gs} - \gamma_{ls} < \gamma_{gl}$, i.e., $\beta_1 > \mu$, which disagrees with the actual $d=3$ values,⁶⁶ $\mu \sim 1.3$, $\beta_1 \sim 0.8$. This argument is not without its ambiguity: In the completely wet phase $\gamma_{gs} - \gamma_{ls} = \gamma_{gl} \sim t^\mu$, so (46) must fail. This is understandable within a mean-field framework, where $\mu = \frac{3}{2}$, $\beta_1 = 1$, and (46) may be regarded near T_c as describing a metastable incompletely wet phase. However, a scaling generalization of Cahn's argument beyond mean-field theory is really not possible, since for $u < u_c$ ($u > u_c$), the incompletely wet (dry) phase disappears before T_c (see

Figs. 10 and 11) and its properties cannot be scaled as $t \rightarrow 0$. To treat the question further it is useful to work near $\delta u \equiv u - u_c = 0$, $t = 0$, where a scaling description presumably exists. The nearest scaling equivalent of Cahn's argument is then just the statement that the surface field δu is a "relevant" variable^{65,66} in the renormalization-group sense, so

$$\gamma_{gs} - \gamma_{ls} \sim t^{(d-1)\nu} \mathcal{F}(\delta u / t^{\Delta_s^{(0)}}) \quad (47)$$

with

$$\mathcal{F}(x) = \begin{cases} \text{const} \times x & \text{as } x \rightarrow 0 \\ \text{singular} & \text{at } x = x_0 > 0 \\ \text{const} & \text{as } x \rightarrow \infty \end{cases} \quad (48)$$

Behavior as $x \rightarrow 0$ reflects the fact that $\gamma_{gs} - \gamma_{ls}$ vanishes by symmetry⁶⁷ when $\delta u = 0$ and gives $\gamma_{gs} - \gamma_{ls} \sim t^{\beta_1} \delta u$ for fixed $t \neq 0$ as $\delta u \rightarrow 0$. Behavior as $x \rightarrow \infty$ assures $\gamma_{gs} - \gamma_{ls} \sim t^{(d-1)\nu}$ as $t \rightarrow 0$ at fixed $\delta u \neq 0$, which continues to hold even for large substrate fields. The wetting singularity is characterized by what happens at x_0 . It follows from this analysis that

$$|T_c - T_{W,D}(u)| \sim |\delta u|^{1/\Delta_s^{(0)}}, \quad (49)$$

where⁶⁶ $\Delta_s^{(0)} \sim 0.46$ in $d=3$.

The wetting transition has been seen experimentally for several adsorption systems, including⁶⁸ O_2 , ammonia,²⁶ and ethylene^{27,28} on graphite (see Sec. IV). Analogous behavior in three-phase, fluid-fluid-vapor systems was first observed by Heady and Cahn⁵⁸ and has been seen subsequently by several other groups.^{56,57,69} The drying transition has yet to be definitively observed experimentally. Monte Carlo calculations have recently been carried out by Sullivan *et al.*⁵⁹

3. The roughening transition and its influence on singular behavior near wetting and drying transitions

Roughening is primarily an interfacial as opposed to surface phase transition. It shows up as a very weak singularity⁶⁴ in the interfacial free energy associated with symmetry directions, as in $\gamma_{gl}(T, \hat{x})$. The long-wavelength capillary-wave fluctuations which dominate the interfacial wandering in the rough phase are cut off in a film of finite thickness. Thus, a strict roughening transition occurs only when $n_s \rightarrow \infty$ ($n_s \rightarrow -\infty$), i.e., as $\mu \rightarrow \mu_0^-$ ($\mu \rightarrow \mu_0^+$) and for surfaces which are completely wet (dry) at

coexistence. Under these conditions the equality (38) [(39)] holds and $\gamma_{gs}(T)$ [$\gamma_{ls}(T)$] inherits from γ_{gl} the roughening singularity⁷⁰ at $T=T_R$. In addition, the roughening transition at T_R , μ_0^- (μ_0^+) makes itself felt in a qualitative way for $\mu \lesssim \mu_0$ ($\mu \gtrsim \mu_0$) provided $T_W < T_R$ ($T_D < T_R$). The order parameter of the roughening transition is the step energy (or kink mass), which is positive for $T < T_R$, zero for $T > T_R$, and vanishes continuously as $T \rightarrow T_R^-$. It is the nonzero kink energy which allows clean distinction between successive layers in the thick-film limit. Hence, distinct layer transitions leading to complete wetting (drying) can only occur⁵ for $T_W < T < T_R$ ($T_D < T < T_R$), and distinct-layer critical temperatures $T_c(n)$ approach T_R as $n \rightarrow \infty$, as illustrated in Figs. 1 and 2. Note that, unlike T_W and T_D , T_R is independent of the substrate potential $\{u_n\}$. Thus, it is in principle possible experimentally to adjust T_W and T_D relative to T_R by varying substrates with a fixed type of adatoms.

The wetting transition is observed for intermediate substrate strengths $u_W < u < u_c$ (Figs. 10 and 11) and its character depends crucially on the relative positions of $T_W(u)$ and T_R . If $0 < T_W < T_R$ (i.e., $u_W < u < u_R$), then, as T increases from zero towards T_W , complete wetting at coexistence is achieved via an infinite sequence of first-order surface-layer transitions which accumulate at T_W (Fig. 2). This is the “layering” subregion identified in Sec. I. When $T_R < T_W$, these layer transitions can no longer remain distinct. The simplest conjecture is that all but a finite number of layer transitions coalesce (at least for $\mu \rightarrow \mu_0^-$) into a single first-order prewetting line (Fig. 3). Precisely such a line is seen in density-functional theory,⁶ continuum mean-field theory,^{13,17,23,71,72} and one Monte Carlo simulation.²⁵ This range of couplings, $u_R < u < u_{CW}$, is the “prewetting” subregion. As the substrate is weakened further, there is plausible but not conclusive evidence that the length of the prewetting line decreases and goes to zero²¹ at a characteristic coupling u_{CW} ($u_R < u_{CW} < u_c$) with $T_{CW} = T_W(u_{CW})$. For substrates weaker than u_{CW} ($u_{CW} < u < u_c$) complete wetting occurs via a second-order “critical wetting” transition. It is not known with certainty that critical wetting persists beyond mean-field theory. In this paper we shall adopt the point of view that it does. Continuum mean-field theory, which cannot describe discrete layering or roughening but might well be expected to be qualitatively valid for $T > T_R$ predicts⁷¹ this changeover from prewetting to critical wetting.

Expected behavior of thermodynamic quantities at coexistence for strong and intermediate substrates is summarized in Fig. 12, which shows sketches of γ_{gs} , γ_{ls} , and $n_s(\mu_0^-)$. Note that the free energies are bounded and continuous as functions of T , in accordance with the discussion after Eq. (17). Near bulk criticality it is natural to suppose that

$$f_s(T, \mu) \sim t^{(d-1)\nu} \mathcal{F}((\mu - \mu_0)/t^\Delta) + \mathcal{B}, \quad (50)$$

where \mathcal{B} is some analytic background, so that, apart from background terms, γ_{gs} and γ_{ls} and their difference γ_{gl} all vary as $t^{(d-1)\nu}$, while $n_s(\mu_0^-)$ diverges for all $T_W < T < T_c$ and varies as $t^{(d-1)\nu - \Delta}$ for $T \gtrsim T_c$. The roughening transition appears as a weak singularity⁷⁰ in γ_{gs} for $T_W < T_R$ but not for $T_W > T_R$. When $0 < T_W < T_R$ [Fig. 12(b)], $n_s(\mu_0^-)$ diverges as T approaches T_W from below via the infinite sequence of layer transitions which accumulate at T_W . In the prewetting subregion [Figs. 3 and 8(c)], we conjecture that $n_s(\mu_0^-)$ goes to a finite value as $T \rightarrow T_W^-$, reflecting our picture of layer-transition coalescence. In the critical-wetting subregion [Figs. 4 and 12(d)] $n_s(\mu_0^-)$ diverges continuously as $T \rightarrow T_{CW}$. To the best of our knowledge the values of the critical exponents describing this divergence and the corresponding singularity in γ_{gs}

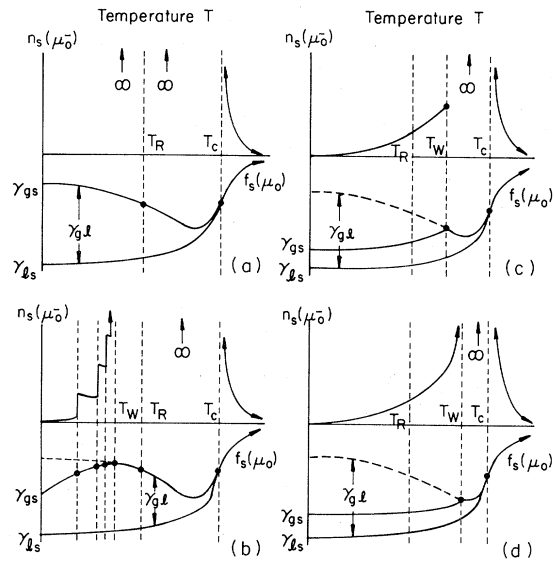


FIG. 12. Sketches of the behavior of the surface coefficients $\gamma_{gs}(T)$ and $\gamma_{ls}(T)$ and the gas-phase excess surface density $n_s(T, \mu_0^-)$ for (a) strong substrate, (b) intermediate substrate, layering, (c) intermediate substrate, prewetting, and (d) intermediate substrate, critical wetting. $f_s(\mu_0)$ is the surface free energy at $\mu = \mu_0$ but for $T > T_c$, beyond coexistence. The enlarged dots show positions of nonanalyticities in the surface coefficients.

have not even been conjectured (for $d=2$ see Appendix B). Also unstudied are the special singularities which occur when $T_W=T_R$ and at the boundary T_{CW} between prewetting and critical wetting.

Behavior in the weak-substrate regime is entirely analogous to behavior in the intermediate-substrate regime by virtue of the (approximate) symmetry about $u=u_c$ (Figs. 10 and 11), only now $\gamma_{gs}(T)$ is smooth for $T < T_c$ and all singularities appear on the liquid side of coexistence. There is “critical drying” for $u_c < u < u_{CD}$ ($T_c > T > T_{CD}$), “predrying” for $u_{CD} < u < u_{\bar{R}}$ ($T_{CD} > T > T_R$), and “layering” for $u_{\bar{R}} < u < 0$ ($T_R > T > 0$).

III. CALCULATIONS AND RESULTS

This section sets forth the evidence for the phase diagrams shown in Figs. 1–6. Beyond the $T=0$ and $\mu=\mu_0$ treatments of Sec. II, it is necessary to rely on approximate and/or numerical techniques. In Sec. III A we review the results of mean-field calculations performed by us⁷¹ and others.^{5,24} Mean-field theory gives a global picture which, although not quantitative, is accurate in some respects: It is exact at $T=0$ and exhibits both layering and wetting. In other ways mean-field theory is completely wrong: It is unable to describe the roughening transition and related phenomena.⁷² Section III B discusses the modification of mean-field results by thermal fluctuations. We concentrate here on a two-dimensional substrate surface in contact with a three-dimensional bulk. The behavior of a one-dimensional substrate in contact with a two-dimensional bulk is treated in Appendix B. In this case mean-field theory does not provide an adequate starting point; however, all the interesting behavior occurs at $T=0$ and $\mu=\mu_0$, so it is possible to form a complete picture.

A. Mean-field results

Mean-field calculations for the discrete lattice-gas model (3) were first carried out for a strong substrate potential of the form (6) by de Oliveira and Griffiths.⁵ Similar calculations for a weaker substrate were recently performed by Ebner.²⁴ We have studied⁷¹ the particularly simple case of nearest-neighbor-only interactions (8) systematically over a range of ratios u/v . The methodology of such mean-field calculations has been adequately expounded in the literature.^{5,24,72} We shall first present results for the nearest-neighbor model and

then discuss in less detail how such results are modified by further-neighbor interactions.

For nearest-neighbor-only interactions, (8) and (12), several exact results are available. The $T=0$ analysis of Sec. II B and Appendix A identifies $u_W=v$. For $u < v$ (i.e., $|u| > |v|$, the strong-substrate regime) the first layer forms on the substrate at $T=0$ when $\mu_0 - \mu = v - u$. At $T=0$ all further layers form simultaneously at $\mu_0 - \mu = 0$. In addition, the magnetic symmetry (12)–(14) means that the nearest-neighbor-only model is exactly symmetric about $u = u_c = \frac{1}{2}v$, $\mu = \mu_0$, so it is only necessary to study the strong ($u < v$) and intermediate ($v < u < \frac{1}{2}v$) regimes. Properties in the weak ($\frac{1}{2}v < u < 0$) regime follow by symmetry from those in the intermediate regime (e.g., Fig. 6). These exact relations are respected by mean-field theory. For the nearest-neighbor simple-cubic lattice mean-field theory gives $k_B T_c = \frac{3}{2} |v|$.

Figure 13 shows representative (μ, T) and (n_s, T) mean-field phase diagrams for $u/v = 1.25$, 0.975, and 0.025. Note that the $u/v = 0.975$ and 0.025 data are related by $\mu - \mu_0 \leftrightarrow \mu_0 - \mu$ and $n_s \leftrightarrow -n_s$.

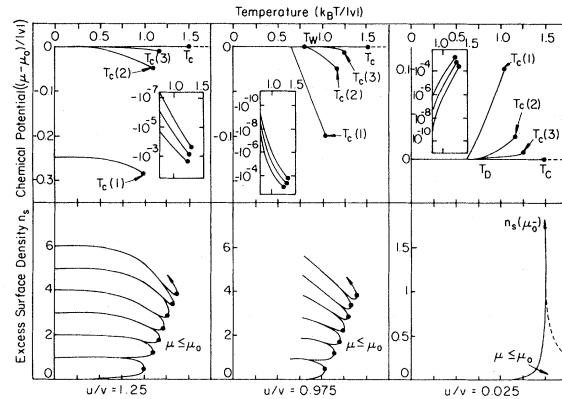


FIG. 13. Representative T, μ and T, n_s mean-field phase diagrams for the simple-cubic nearest-neighbor model (8) for $u/v = 1.25$ (strong substrate), $u/v = 0.975$ (intermediate substrate, $k_B T_W / |v| \simeq 0.78$), and $u/v = 0.025$ (weak substrate, $k_B T_D / |v| \simeq 0.78$). There is an infinite sequence of layer transitions, with $T_c(n) \rightarrow T_c$ (bulk) as $n \rightarrow \infty$. Only the transitions $n = 1, 2$, and 3 are actually shown on the T, μ surface phase diagrams ($n = 4, 5$, and 6 are shown on the semilogarithmic insets). Because of the exact magnetic symmetry the T, μ phase diagrams for $u/v = 0.975$ and 0.025 are mirror images. It is a special feature of the nearest-neighbor model that only a single layer transition separates off at $T=0$ in the strong regime. The T, n_s phase diagrams exhibit the excess surface density along the phase boundaries, including coexistence. Allowed regions connect to the lower right.

Within the context of discrete mean-field theory these phase diagrams are qualitatively typical of all behavior⁷³ in the strong, intermediate, and weak regimes, respectively. Consider first the (μ, T) phase diagrams. The sequence of phase boundaries approaching the coexistence axis represents successive layer transitions, $n=1,2,3,\dots$. For $u/v > 1$ all layer transitions reach $T=0$, with coincidence at $T=0$ of all the layers $n > 1$. This coincidence is an exact consequence of the choice of nearest-neighbor interactions. For $\frac{1}{2} < u/v < 1$ the layer transitions, separated now by entropy contributions, reach $\mu=\mu_0$ (coexistence) at distinct temperatures, which accumulate as $n \rightarrow \infty$ at the wetting temperature T_W . Each layer transition n terminates at a critical temperature $T_c(n)$. Because of its failure to include roughening, mean-field theory (incorrectly) predicts $T_c(n) \rightarrow T_c(\text{bulk})$ as $n \rightarrow \infty$ (although the approach to this limit is rather slow). Thus, for $n \rightarrow \infty$ the layer-transition lines approach the segment of the coexistence axis between T_W and T_c . In the weak regime $0 < u/v < \frac{1}{2}$ all the layer transitions have shifted to the liquid side of coexistence. The (n_s, T) phase diagrams of Fig. 13 plot the excess surface density versus temperature for points along the phase boundaries⁷⁴ on the gas side of coexistence. The fingerlike shapes are regions of coexistence of the two surface phases (of different n_s but at the same T) on opposite sides of the (μ, T) layer-transition phase boundaries. For $u/v > 1$ the fingers extend down to $T=0$, join at a cusp there, but are separated⁷⁵ at $T > 0$ by narrow regions of allowed, single-phase n_s . For $\frac{1}{2} < u/v < 1$ fingers join⁷⁶ at $T > 0$. The points of joining approach T_W as $n_s \rightarrow \infty$ at wetting. For $0 < u/v < \frac{1}{2}$ there are no gas-phase layer transitions and $n_s(T, \mu_0^-)$ changes continuously along the coexistence curve, diverging as $|\ln t|$ as $T \rightarrow T_c^\pm$.

Representative adsorption isotherms and “isobars”⁷⁷ are shown in Fig. 14 for some of the same data as Fig. 13. Both isotherms and isobars exhibit sharp steps at the layer transitions. When the substrate is completely wet at coexistence (within mean-field theory this occurs for $0 < T < T_c$ for $u/v > 1$ and $T_W < T < T_c$ for $\frac{1}{2} < u/v < 1$), the corresponding isotherms show an infinite sequence⁷⁸ of such steps as $\mu \rightarrow \mu_0^-$. The approximately equal horizontal length of these steps in Fig. 14 reflects the logarithmic behavior of $t(T, \mu)$ expected for short-ranged potentials [see after Eq. (42)]. Of course, for $0 < T < T_W$ at most a finite number of steps is present. The isobars at $\mu < \mu_0$ show a finite number of steps followed by a smooth decay to-

wards zero for $T > T_c$. As $\mu \rightarrow \mu_0^-$ the isobars should in principle approach those shown in Fig. 12. For $u/v > 1$ [Fig. 12(a)] this does, in fact, happen; however, for $\frac{1}{2} < u/v < 1$ all curves approach the limiting form of Fig. 12(b), so Figs. 12(c) and 12(d) are never seen, reflecting, again, the absence of a roughening transition in mean-field theory. Nevertheless, it is interesting to note that for weaker substrate potentials (e.g., $u/v=0.75$ in Fig. 15) the horizontal size of the steps becomes very small and prewetting—critical-wetting behavior is simulated at a gross level.

Inclusion of further-neighbor attractions^{5,24} modifies the nearest-neighbor-only picture presented above in two important ways: (i) Successive layer transitions are separated at $T=0$ (cf. Fig. 13) and (ii) surface triple points may occur. Both these modifications may be studied exactly at $T=0$ in the strong-substrate regime [Sec. II, Eq. (27)ff, and Appendix A]. The first corresponds to the separation and orderly sequencing of the chemical potentials at which the successive $T=0$ layer transitions occur, $\mu_1 < \mu_2 < \dots < \mu_0$; the second, to the possibility for sequencing of the type $0, 1, \dots, n, n+q, n+q+1, \dots$, liquid, in which several layers

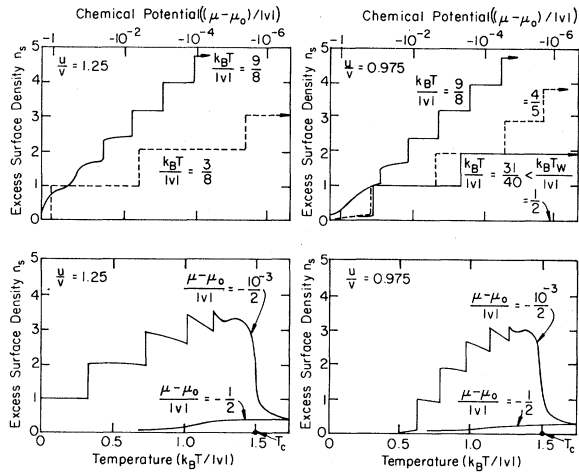


FIG. 14. Representative mean-field gas-phase adsorption isotherms $n_s(\mu)$ and “isobars” $n_s(T)$ for the same data as Fig. 13. In the strong-substrate regime ($u/v = 1.25$) all isotherms are class I; however, at higher temperatures the first few layer transitions are rounded because $T > T_c(1)$, etc. In the intermediate-substrate regime the isotherms are class II for $T < T_W$ and class I for $T_W < T < T_c$ (for $u/v = 0.975$, $k_B T_W/|v| \simeq 0.78$). The isobars are smooth except when they cross a phase boundary. As μ approaches μ_0^- , more and more such boundaries are crossed. The height of the peak diverges as $|\ln(\mu_0 - \mu)|$ [see after Eq. (42)].

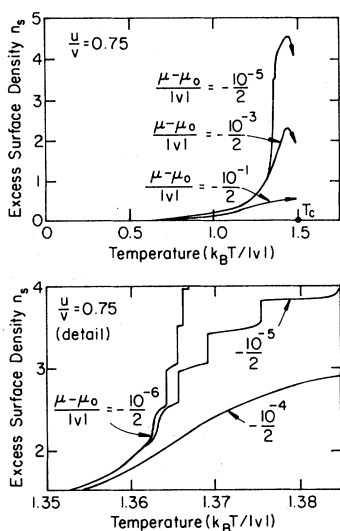


FIG. 15. Mean-field gas-phase adsorption isobars for $u/v=0.75$, in the intermediate-substrate regime. Observed at a fine scale (see detail), these isobars are similar to those shown in Fig. 14; however, on a coarse scale they exhibit the kind of smooth behavior expected in the prewetting subregion. For $u/v=0.75$, $k_B T_W / |v| \approx 1.36$.

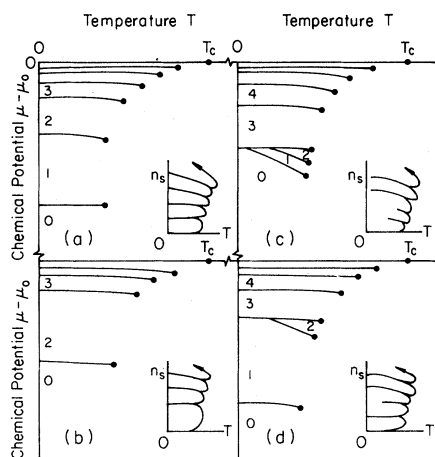


FIG. 16. Possible mean-field surface phase diagrams for strong-substrate systems with further-neighbor interactions. Longer-ranged interactions separate the layer transitions at $T=0$. A potential [e.g., Eq. (6)] which decays strongly and monotonically separates all layer transitions, as in (a). When two or more layers feel potentials which are nearly the same, their transitions may occur simultaneously at $T=0$ [(b)–(d)]. In solved examples with weaker substrates (Ref. 79) the transitions tend to separate off at higher temperature via surface triple points [(c) and (d)]; however, it is not known whether this always happens [c.f. (b)]. In all cases $T_c(n) \rightarrow T_c(\text{bulk})$ as $n \rightarrow \infty$.

fill together. Monotonically decreasing substrate potentials which are strong enough to wet at $T=0$ lead to sequential layer filling, $0, 1, 2, \dots$, liquid, when the layer potential falls off rapidly, thus cleanly distinguishing layer n from layer $n+1$ [see Eq. (30)]. Conversely, several layers which feel more or less the same substrate potential may fill together. Layers which fill together at $T=0$ may be separated by entropy effects at T increases, thus leading to triple points. Corresponding effects are also expected for intermediate and weak substrates. Examples of the various different types of phase diagrams which may be expected are shown in Figs. 16 and 17. Only a few of these have yet been seen⁷⁹ for the small number of potentials that have been studied explicitly. Note that in all cases $T_c(n) \rightarrow T_c$ as $n \rightarrow \infty$.

The major qualitative defect of mean-field theory is its failure to include roughening and the consequent absence of prewetting and critical-wetting phenomena. For short-range forces $T_R \sim \frac{1}{2} T_c$, so we may say crudely that discrete mean-field theory gives a reasonable description at low temperatures but not at high temperatures. Surface phenomena have also been treated by continuum mean-field theories.^{6,13,17,23,71} Indeed, it was from this point of

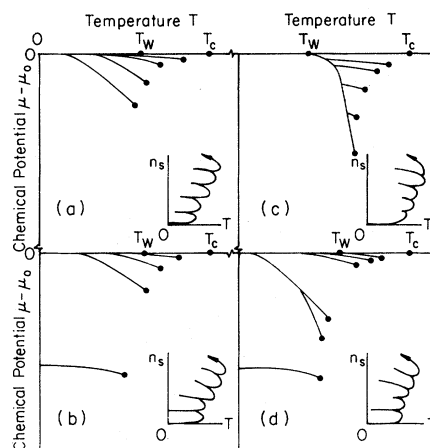


FIG. 17. Possible mean-field surface phase diagrams for intermediate-substrate systems with further-neighbor interactions. Interactions of relatively short range appear to lead to phase diagrams such as (a) [e.g., Fig. 13]. Strong first-layer interactions can split off one (or more) separated layer transitions as in (b). Longer-ranged interactions appear to lead (Ref. 79) to a series of surface triple points (c). There is no reason to believe that additional composite and/or intermediate cases do not occur [e.g., (d)]. As in Fig. 16, $T_c(n) \rightarrow T_c(\text{bulk})$ as $n \rightarrow \infty$. Corresponding phase diagrams for the weak-substrate regime are simply inverted in the T axis (Fig. 13), so $\mu - \mu_0 \leftrightarrow \mu_0 - \mu$ and layer transitions take place in the bulk-liquid region.

view that both prewetting and critical wetting were first discovered (see Sec. IIC2). The applicability of continuum mean-field theories is somewhat ambiguous: Discrete-layer transitions are not possible. Such theories are arguably valid (i) for $T > T_R$, where layer transitions are absent anyway, and (ii) in some lumped, average sense over the full phase diagram; however, they can certainly not shed any light on the complicated questions surrounding the crossing of T_W and T_R . Nevertheless, Sullivan's theory,²³ valid in sense (ii) above, is the first and until now only treatment of the crossover from class-II to class-I behavior as a function of T and the ratio u/v .

B. Beyond mean-field theory

For $T > 0$ the results of mean-field theory are modified by the presence of thermal fluctuations. These fluctuations have a disordering effect and tend to reduce (often substantially) the temperatures at which ordering phenomena occur. Of course, they also modify the details of critical behavior near second-order phase transitions, both bulk and surface. From a global point of view the main consequence of including thermal-fluctuation effects is to produce the interfacial roughening phenomena described in Sec. IIC2. Interfacial roughening becomes a *surface* phenomenon only in the strict thick-film (complete-wetting) limit; however, associated qualitative effects extend away from coexistence. Thus, the considerations of Sec. IIC allow a satisfactory *qualitative* description of adsorption systematics beyond mean-field theory. Numerical evidence to support this description is sparse at present: There are Monte Carlo simulations by Ebner²⁵ and by Kim and Landau⁸⁰ and, most recently, a Migdal-Kadanoff renormalization-group calculation by Saam⁸¹ for four- and five-layer lattices. What evidence there is is consistent with the picture we now present.

Possible phase diagrams for $u \ll u_W$ (strong substrate, complete wetting at coexistence) are shown in Fig. 18. For nearest-neighbor interactions only [Fig. 18(a)] the $n > 1$ layer transitions bunch at $T = \mu - \mu_0 = 0$. A long-ranged but rapidly decreasing substrate potential [Fig. 18(b), which is identical to Fig. 1] separates the layer transitions at $T = 0$. Weaker falloff and further-neighbor particle-particle interactions can lead to multiple-layer transitions and triple points, just as within mean-field theory. The qualitative difference between Fig. 16

(and Fig. 13, $u/v=1.25$) and Fig. 18 is that now $T_c(n) \rightarrow T_R$ as $n \rightarrow \infty$, reflecting the influence of roughening on the completely wet substrate at coexistence. Phase diagrams such as Fig. 18(b) have been seen in Monte Carlo simulations.^{25,80} Note that Fig. 18 shows $T_c(n)$ increasing with n , as has been observed in the simulations. This tendency is certainly nonuniversal, at least for small n , in that it must depend on the details of the substrate potential in the first few layers.⁸² The experimental situation appears correspondingly variable.⁸³

Intermediate substrates, $u_W < u < u_c$, have a nonzero wetting temperature, $0 < T_W < T_c$, and divide into three subregions, layering, prewetting, and critical-wetting, as described in Secs. I and IIC. In the layering subregion, $u_W < u < u_R$, $0 < T_W < T_R$, the situation is as shown in Fig. 19 (see also Fig. 2), which should be compared to Fig. 17, the corresponding mean-field results. Again, roughening controls the thick-film behavior, so $T_c(n) \rightarrow T_R$. Note that a substrate potential which is strong in the first few layers but weak thereafter can split one or more layer transitions away from the coexistence axis [Fig. 19(b)], so the isotherms contain one or more steps at arbitrarily low temperature, despite being class II for all $T < T_W$.

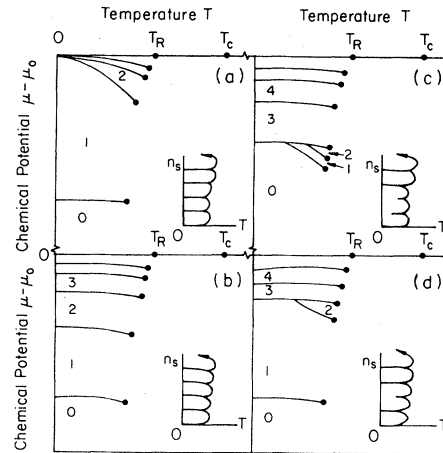


FIG. 18. Surface phase diagrams beyond mean-field theory, strong-substrate regime, $u < u_W < 0$. For short-ranged interactions [e.g., nearest neighbor, as in (a)] layer transitions are bunched at $T = 0$. Longer-ranged interactions with rapid falloff separate the transitions at $T = 0$ [e.g., (b)]. If interactions in the first few layers are closely matched, surface triple points may occur (c). A particularly strong first-layer interaction splits away the first-layer transition (d). In all cases $T_c(n) \rightarrow T_R$ as $n \rightarrow \infty$, as originally argued in Ref. 5.

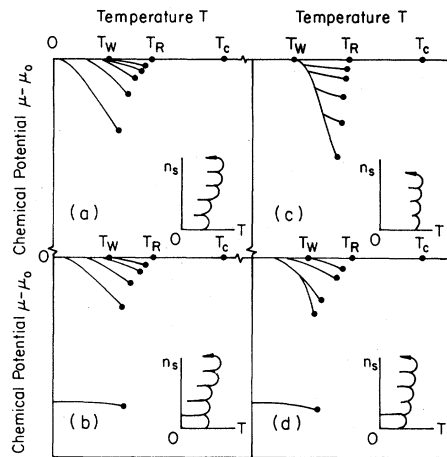


FIG. 19. Surface phase diagrams beyond mean-field theory, intermediate substrate regime, prewetting subregion, $u_W < u < u_R < 0$. Here $0 < T_W < T_R$ and the layer-transition temperatures $T_c(n)$ approach T_R as $n \rightarrow \infty$. Short-ranged substrates probably leave layer transitions distinct as in (a). Particularly strong early-layer interactions may split off one or more transitions onto the $T=0$ axis [(b) and (d)]. Longer-ranged interactions may give a sequence of surface triple points (c). Intermediate and mixed situations (d) may presumably occur for appropriate substrates. T, μ phase diagrams for the weak-substrate regime are obtained by inverting $\mu - \mu_0 \leftrightarrow \mu_0 - \mu$ in the coexistence axis, so that $T_W \leftrightarrow T_D$ and layering takes place on the liquid side of coexistence.

Whether layer transitions are always separate and distinct, as in Figs. 19(a) and 19(b), or merge via surface triple points, as in Fig. 19(c), is not possible to determine without detailed calculations, which have not yet been done. Within mean-field theory, nearest-neighbor-only interactions lead to separate transitions (Fig. 13), while longer-ranged interactions can give triple points.²⁴ It is, therefore, plausible to suppose that appropriate potentials can produce both types of behavior and, indeed, other intermediate cases such as Fig. 19(d). The common features of all variants of this phase diagram are class-II isotherms for $T < T_W$ and class-I isotherms for $T_W < T < T_C$, thus allowing situations in which increasing temperature *increases* the number of layer transitions seen. Just such behavior has been clearly observed by Menaucourt^{27,28} for ethylene on graphite, as we shall discuss more fully in Sec. IV. Indeed, it is a consequence of the Cahn argument¹³ (see Sec. II C 2) that *any* system exhibiting class-II isotherms will eventually develop class-I isotherms as T is increased, so this kind of behavior is probably common.

Weakening the substrate potential still further

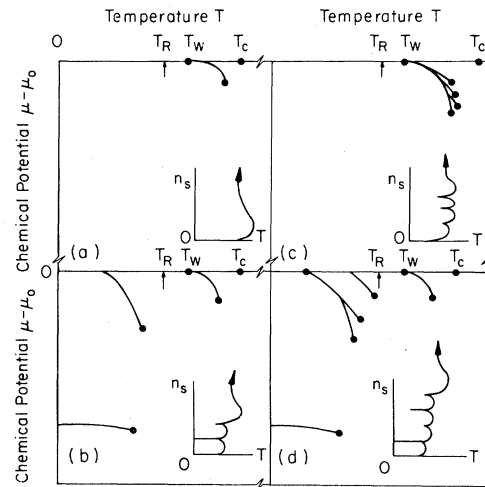


FIG. 20. Surface phase diagrams beyond mean-field theory, intermediate substrate regime, prewetting subregion, $u_R < u < u_{CW} < 0$. When T_W is above T_R , high-order layer transitions cannot remain distinct at coexistence. There is no longer any thick-film behavior at coexistence near T_R , so roughening singularities disappear from the surface problem. For some interactions, the prewetting line appears to be simple as in (a) (Ref. 25); however, early layers may be split off as in (b) and (d). There seems no reason in principle to exclude surface triple points away from coexistence [(c) and (d)]. Similar behavior in the predrying subregion for weak substrates is obtained by reflecting $\mu - \mu_0 \leftrightarrow \mu_0 - \mu$ and $T_W \leftrightarrow T_D$.

raises T_W above T_R . Figure 20 (see also Fig. 3) depicts possible phase diagrams in the prewetting subregion, $u_R < u < u_{CW}$, $T_R < T_W < T_{CW}$. Corresponding pictures for the critical-wetting subregion, $u_{CW} < u < u_c$, $T_{CW} < T_W < T_c$, lack the prewetting phase boundary but are otherwise the same (e.g., Fig. 4). Because thick films occur only at temperatures above T_R , the point $T = T_R$, $\mu = \mu_0$ is no longer special and the sequence of distinct layer transitions leading to complete wetting for $T_W < T_R$ (Fig. 19) coalesce in the prewetting subregion into a single thick-film – thin-film prewetting line, at least near coexistence. Ebner's Monte Carlo simulations²⁵ appear to show a phase diagram like Fig. 20(a) for a particular 3–9 potential. Note that a strong substrate potential in the first few layers can still split off a *finite* number of layer transitions below T_R [Figs. 20(b) and 20(d)]. Away from coexistence there is nothing in principle to prevent layer transitions, surface triple points, etc., as sketched in Figs. 20(c) and 20(d). In the critical-wetting subregion the prewetting line shrinks to a single point on the coexistence axis (see Sec. II C 2); however, finite numbers of layer transitions may presumably per-

sist elsewhere in the phase diagram (away from $\mu = \mu_0$, $T > T_R$) for suitable potentials. Which of these many possibilities is realized for a particular combination of atom-atom and atom-substrate potentials can only be determined by detailed calculations, as yet unavailable.

Possible phase diagrams for the weak-substrate regime are obtained from those in the intermediate-substrate regime (Figs. 19 and 20) by reflecting all phase boundaries onto the liquid side of coexistence. The discussion parallels that given above with drying substituted for wetting, $T_W \leftrightarrow T_D$, etc.

IV. DISCUSSION: THE LATTICE MODEL VERSUS EXPERIMENT

A. Deficiencies of the lattice-gas model

The lattice-gas model (3) does have a bulk first-order transition from a low-density (gas) phase to a high-density (liquid) phase which ends at a critical point possessing the experimentally correct liquid-gas critical exponents; however, as a description of the real world, it is at best only partially successful. Some of its deficiencies are rather subtle (e.g., the “magnetic” symmetry of the associated Ising model artificially straightens out the coexistence-curve diameter⁸⁴) and others refer to regions of extreme temperature or pressure, beyond the principal focus of our present concerns (e.g., it is a “classical” model and cannot describe quantum effects, which may become important at very low temperatures). Others, however, are grossly evident in regions of major experimental interest. We shall concentrate on four interrelated problems.

1. Lack of a solid phase

The lattice-gas model has only two bulk phases, which meet along a single coexistence line. By contrast, even simple materials such as the rare gases (helium excepted) have a bulk phase diagram [Fig. 21(a)] with three bulk phases, meeting along three distinct coexistence lines which join at a bulk triple point. Even if we confine ourselves to those situations (which have received almost all experimental attention) where one of the coexisting phases is the gas, there is still a new characteristic temperature, the triple-point temperature T_t , which must play an important role in the coexistence analysis of Sec. II C. Along the liquid-gas boundary the two coexisting phases are both continuum phases, so the in-

terface is always rough.⁸⁵ Thus, there are two possibilities⁸⁶: Either there is an ordinary roughening transition along the gas-solid coexistence line, $0 < T_R < T_t < T_c$, or there is no roughening transition in the usual sense but simply a transition at T_t between a smooth gas-solid interface and a rough gas-liquid interface. In the former case our previous discussion applies directly and T_t is unimportant. In the latter case the triple point must play the same role as the roughening transition in bounding the critical temperatures $T_c(n)$, above which layer transitions cannot remain distinct for large n . Otherwise, the systematics of surface transitions in the bulk-gas region should not be substantially influenced [see Figs. 21(b)–21(d)] by the presence of the additional high-density phase. It seems likely that the situation for O_2 on graphite^{68,83} is of this type [probably Fig. 21(c)].

The free energy f_s and corresponding surface coefficients will, of course, have singular behavior near T_t . When $T_W < T_t$, so that complete wetting occurs near the triple point, then in analogy to (38),

$$\gamma_{\text{gas-substrate}} = \gamma_{\text{solid-substrate}} + \gamma_{\text{gas-solid}} \quad \text{for } T_W \leq T \leq T_t \quad (51a)$$

and

$$\gamma_{\text{gas-substrate}} = \gamma_{\text{liquid-substrate}} + \gamma_{\text{gas-liquid}} \quad \text{for } T_t \leq T \leq T_c \quad (51b)$$

At the triple point $\gamma_{\text{gas-substrate}}$ is continuous and both equalities hold; however, there seems no reason not to expect discontinuity in slope. On the other hand, when $T_W > T_t$, then thick films cannot occur as gas-solid coexistence is approached from the gas phase, so at $T = T_t$, $\mu \rightarrow \mu_0^-$ surface thermodynamic functions should inherit only the very weak coexistence-curve singularities⁸⁷ characteristic of the bulk; however, the coexistence “crystallites” which grow at $\mu = \mu_0$ change shape discontinuously across T_t from anisotropic ($T < T_t$) to spherical ($T > T_t$). Of course, special singular behavior is presumably expected for $T_R = T_t$, $T_W = T_t$, or both.

2. Monolayer structure, epitaxial transitions

For the purely attractive interactions which we have studied, each layer transition involves the condensation of a low-density ($d=2$ gas) phase into a high-density ($d=2$ liquid) phase. This simple two-phase picture may be adequate for high-order-layer

transitions but is certainly inadequate to describe the rich diversity of experimental monolayer and bilayer structure. Purely epitaxial effects are discussed here; those involving incommensurate phases and/or situations with serious misfit between the substrate and the bulk adatom solid are discussed in the next subsection. In nature both effects can and do occur together.

The appearance of epitaxial ordering, such as in the $\sqrt{3} \times \sqrt{3}$ phase,¹ typically requires atom-atom forces with competition between, for example, nearest-neighbor repulsion and further-neighbor attraction. Such effects can be modeled with a lattice gas and form the subject of a separate publication.⁸⁸ If repulsion is weak, then at each temperature the epitaxial phase exists only over a narrow range of density (chemical potential) and the addition of further adatoms completes the layer, destroying epitaxial order. Thus, single-line layer-transition phase boundaries in the (μ, T) plane open up into narrow "fingers" bounding regions of epitaxial order. At the opposite extreme, strong repulsion may prevent completion of the first layer. Then, the second and subsequent layers condense *in registry* under an envelope of epitaxy in the (μ, T) plane. In both limiting situations the general systematics of layer condensation should be as described in the text.

3. Imposed versus spontaneous lattice structure, incommensurate phases

Incommensurate phases and the transitions between commensurate and incommensurate phases cannot, of course, be described adequately by a lattice-gas model with attractive interactions. Such effects *must* be felt in the process of building up thick films in the vicinity of the bulk gas-solid phase boundary, unless the adatom solid phase is precisely commensurate with the substrate surface. Incommensurate ($d=2$ solid) phases often occur for early ($n=1,2$) layers and certainly render the description of such layers beyond our model; however, it seems likely that the effect of these early layers on the large- n systematics is small: Near the bulk gas-liquid phase boundary ($\mu \rightarrow \mu_0^-$, $T_t < T < T_c$) the high- n layers are more or less uniform and should admit a lattice-gas description, while near the bulk gas-solid phase boundary ($\mu \rightarrow \mu_0^-$, $0 < T < T_t$) the high- n layers (beyond some characteristic "healing" distance) will have essentially the bulk-solid lattice structure.

4. Weak-substrate layering

Note finally that the layering transitions on the *dense*-phase side of coexistence which are present in the lattice gas (weak substrate, layering subregion) are an artifact of the model and not to be expected in the real world.⁸⁹ For a weak substrate and in the dense bulk phase the "film" is actually a *low*-density region sitting between the substrate surface and the high-density bulk. This film may possibly have thick-thin (predrying-type) transitions; however, it will not have a *sequence* of layer transitions. The physics of this situation is misrepresented by the lattice-gas model. Layering in ordinary, dense films is driven by the hard-core atom-atom repulsion, represented in the model quite appropriately by the lattice; however, at low densities the hard-core repulsion should not play an important role and is artificially overemphasized in the model by the latticization of empty space. These remarks apply most directly to the solid side of the bulk gas-solid phase boundary [Fig. 21(a)]. The point is moot on the liquid side of the gas-liquid phase boundary, since this boundary is rough for all $T_t < T < T_c$. It is not clear what happens near (smooth portions of) the bulk liquid-solid phase boundary, since here both phases are typically dense and hard-core repulsion certainly plays a role.

In summary, then, we anticipate that the simple lattice-gas model we have studied should provide an adequate description of thick-film systematics in the bulk-gas region, though it is bound to miss structural details of the first few layers, if epitaxial and/or commensurate-incommensurate ordering occurs.

B. Implications for and comparison with experiments

To study experimentally the kind of global-phase-diagram systematics on which we have focused, it is necessary to have data at a variety of temperatures T and bulk densities n_b (or, equivalently, chemical potentials μ), e.g., isotherms taken systematically over a wide range of temperatures. In addition, the limitations mentioned in Sec. IV A put a premium on data near coexistence, especially in thick-film regions. For a variety of experimental reasons¹ such data are not easy to gather. In particular, low-temperature work (needed to distinguish between strong and intermediate substrates, Figs. 18–20) involves long equilibration times and thick-film work (needed to distinguish class-I and

class-II isotherms) involves difficulties with capillary condensation and requires good pressure resolution. In view of the above it is, perhaps, not surprising that there does not seem to be even one system for which the full (T, μ) surface phase diagram can be reconstructed in detail from experiments. (Indeed, it is one of our purposes to stimulate interest in what we believe to be a fertile area for new experiments.) Furthermore, qualitative comparison with specific systems which have been studied experimentally, although not out of the question,²³ is hampered by limited knowledge of many atom-substrate potentials and by the difficulty of reliable calculations beyond mean-field theory.

We restrict our remarks, therefore, to some rather broad and qualitative points. The theory predicts⁹⁰ the following:

(i) A system with class-I isotherms at low temperatures will have class-I isotherms at all higher temperatures. Such behavior is to be expected for strongly attractive substrates.

(ii) A system with class-II isotherms at some temperature T_0 will remain class II for all temperatures lower than T_0 ; however, it may ($u < u_c$) or may not ($u > u_c$) shift to class-I behavior in an interval T_W to T_c for some $T_0 < T_W < T_c$. Such behavior is to be expected for intermediate or weak substrates, respectively.

(iii) An infinite sequence of distinct, sharp layer transitions, terminating in critical temperatures $T_c(n)$ is to be expected for all strong and some ($u < u_R$) intermediate substrates. The limit as $n \rightarrow \infty$ of $T_c(n)$ should be either the triple-point temperature T_t or some roughening temperature $0 < T_R < T_t$.

(iv) For potentials of intermediate strength but near u_c ($u \lesssim u_c$) prewetting and, possibly, critical wetting should be seen.

A classic example of the infinite sequence (iii) (actually 5–6 layers) is the Kr-on-graphite work of Singleton and Halsey⁹¹ and more recently of Thomy and Duval.^{92,93} Good data showing class-I isotherms are also available for CH_4 (Ref. 93), Ar (Ref. 94), and O_2 (Ref. 68) on graphite. These data are not inconsistent⁸³ with acceptable limiting values of $T_c(n)$ as $n \rightarrow \infty$. Both O_2 (Ref. 68) and N_2 (Ref. 95) on graphite appear to have class-II isotherms at low T and, thus, to belong to the intermediate-substrate class [Figs. 19 and 21(c)]. To the best of our knowledge it is not known experimentally whether Ar and Kr on graphite remain class I at low T or switch⁹⁶ to class II. ^4He on graphite is known to be class II at low temperatures near the

liquid-gas phase boundary⁹⁷; very recent work⁹⁸ near the liquid-solid phase boundary indicates class-I behavior at 1 K but does not go to lower temperatures.

Several systems are now known with behavior of type (ii), exhibiting, as T is increased, an *increasing* number of sharp layer transitions in the isotherms and, thus, corresponding to intermediate substrate strength. In addition to O_2 mentioned above, recent studies of both ammonia²⁶ and ethylene^{27,28} on graphite show this behavior. The case of ethylene is particularly striking, exhibiting an isotherm with one step at 77 K, two steps at 91 K, and three or more steps at 106 K. The 77- and 91-K isotherms are clearly class II, while the 106-K isotherm appears distinctly class I, indicating that T_W is quite close to T_t (104 K).

Clean instances of prewetting or critical wetting do not yet appear in the literature with which we are familiar. Similarly, although there are many systems showing for particular T isotherms with no measurable adsorption right up to coexistence (Dash's class III, which we regard as "strong" class II), systematic studies have not been made to check whether crossover to class I occurs at higher temperatures. Thus, there are several good candidates

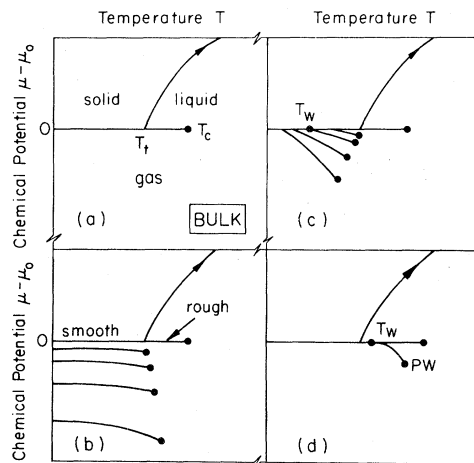


FIG. 21. Phase diagrams for a three-phase system with a bulk triple point. (a) Bulk phase diagram. (b)–(d) Surface phase diagrams, when the gas-solid interface is always smooth, so T_t plays the role of a roughening temperature. (b) Strong-substrate, behavior. (c) Intermediate substrate, layering subregion. (d) Intermediate substrate, prewetting subregion. The intermediate substrate with critical wetting and the various weak-substrate regimes are direct extensions. Of course, variants with split-off layers, surface triple points, etc., are also possible. There is some evidence that O_2 on graphite may be represented by (c).

for weak-substrate behavior (e.g., H₂O on graphite⁶⁰ or, indeed, the familiar mercury on glass) but no confirmed examples. Drying phenomena—complete or incomplete—have not yet to our knowledge been studied experimentally. Standard thermodynamic methods¹ do not lend themselves to detection of a *low*-density surface region against a *high*-density bulk background. Direct measurement of the density profile $n(z)$ would appear to be required.

ACKNOWLEDGMENTS

We are grateful to J. G. Dash, M. den Nijs, C. Ebner, M. E. Fisher, R. B. Griffiths, E. H. Hauge, J. S. Langer, H. Nakanishi, R. E. Peierls, C. Rottman, D. Siebert, J. D. Weeks, and B. Widom. One of us (M.W.) particularly wishes to express his indebtedness to J. G. Dash, without whose unflinching wisdom, friendship, and persistence this paper would have been less complete, less physical, and certainly less enjoyable to write. This work was supported in part by the National Science Foundation under Grants Nos. DMR77-23999, DMR78-21069, DMR79-20785, and DMR81-17182.

APPENDIX A: SURFACE BEHAVIOR AT $T=0$

For given atom-atom and atom-substrate potentials the $T=0$ calculation of $f_s(T=0, \mu)$ outlined in Sec. II B can be done explicitly. To provide a concrete example, we consider below the case of a long-ranged, attractive, monotonic atom-substrate potential,

$$u_1 < u_2 < u_3 < \dots < 0, \quad (\text{A1})$$

subject to the convergence condition⁹⁹

$$\left| \sum_{m=1}^{\infty} u_m \right| < \infty, \quad (\text{A2})$$

and a short-ranged attractive atom-atom potential,

$$v_n = 0 \quad \text{for } n > 2. \quad (\text{A3})$$

1. Nearest-neighbor atom-atom attraction:

$$v_1 < 0, \quad v_2 = 0$$

The minimization (21a) required to compute $f_s(T=0, \mu)$ for $\mu < \mu_0$ (gas phase) is illustrated in Fig. 22. For $n > 0$, the plot of $\frac{1}{2}E_n^{(g)}(\mu)$ [Eq. (19a)]

is a straight line of slope $(-n)$. The local sequencing condition (30) reduces for $n > 1$ to $u_{n+1} - u_n > 0$, which is always satisfied by virtue of the monotonicity of $\{u_m\}$. For $n=0$, $\frac{1}{2}E_0^{(g)}(\mu) = 0$. The function $f_s(T=0, \mu)$ for $\mu < \mu_0$ is by (21a) just the convex envelope of Fig. 22 and is, therefore, composed of a sequence of straight-line segments from the various curves $\frac{1}{2}E_n^{(g)}(\mu)$. The layering sequence as μ increases from $-\infty$ can be read off directly. There are three different types of sequencing possible ($l \equiv$ liquid): The sequence $[0, 1, 2, \dots, \infty, l]$ requires

$$u_1 - u_2 < v_1. \quad (\text{A4})$$

The sequence $[0, n, n+1, \dots, \infty, l]$ for $n > 1$ requires

$$\sum_{m=1}^n u_m - nu_{n+1} < v_1 < \sum_{m=1}^{n-1} u_m - (n-1)u_n. \quad (\text{A5})$$

And, the sequence $[0, l]$ requires

$$v_1 < \sum_{m=1}^{\infty} u_m. \quad (\text{A6})$$

Note that (A4) and (A5) correspond to a strong substrate, with a class-I isotherm at $T=0$, while (A6) corresponds to an intermediate or weak substrate, with a class-II isotherm at $T=0$.

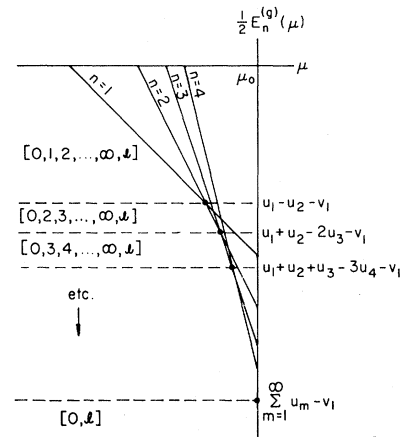


FIG. 22. The surface free energy $f_s(T=0, \mu)$ for $\mu \leq \mu_0$ with monotonically decaying substrate interactions and nearest-neighbor atom-atom interactions. The minimization (21a) requires taking the lowest point at each value of μ . The curve $\frac{1}{2}E_0^{(g)}(\mu)$ is a horizontal line. When $\frac{1}{2}E_0^{(g)}(\mu) > u_1 - u_2 - v_1$, the layering sequence is $[0, 1, 2, \dots, \infty, l]$. When $\frac{1}{2}E_0^{(g)}(\mu) < \sum_{m=1}^{\infty} u_m - v_1$, the layering sequence is $[0, l]$. Other intermediate cases are indicated. Note that $f_s(T=0, \mu)$ consists of straight-line segments and is convex upwards.

2. Next-neighbor-layer interactions: $v_1 < 0, v_2 < 0$

In this case local sequencing holds automatically only for $n > 2$, so both $\frac{1}{2}E_0^{(g)}(\mu)$ and $\frac{1}{2}E_1^{(g)}(\mu)$ must be treated specially. Otherwise, the calculation proceeds as for the nearest-neighbor case. There are now five generically different types of sequencing possible: The sequence $[0, 1, 2, \dots, \infty, l]$ requires

$$v_1 > u_1 - u_2, \quad v_2 > u_2 - u_3. \quad (\text{A7})$$

The sequence $[0, n, n+1, \dots, \infty, l]$ for $n > 1$ requires

$$\sum_{m=1}^n u_m - nu_{n+1} < v_1 + 2v_2 < \sum_{m=1}^{n-1} u_m - (n-1)u_n$$

and (A8)

$$u_1 - \frac{1}{n-1} \sum_{m=2}^n u_m > v_1 + \left[\frac{n-2}{n-1} \right] v_2.$$

The sequence $[0, 1, n, n+1, \dots, \infty, l]$ for $n > 2$ requires

$$\sum_{m=2}^n u_m - (n-1)u_{n+1} < v_2 < \sum_{m=2}^{n-1} u_m - (n-2)u_n$$

and (A9)

$$u_1 - \frac{1}{n-1} \sum_{m=2}^n u_m < v_1 + \left[\frac{n-2}{n-1} \right] v_2.$$

The sequence $[0, l]$ requires

$$\sum_{m=1}^8 u_m > v_1 + 2v_2$$

and (A10)

$$u_1 > v_1 + v_2.$$

The sequence $[0, 1, l]$ requires

$$\sum_{m=2}^8 u_m > v_2$$

and (A11)

$$u_1 < v_1 + v_2.$$

These results are illustrated in Fig. 23, which shows the regions of different sequencing over the (v_1, v_2) plane for a representative example. Note that the new sequences $[0, 1, n, n+1, \dots, \infty, l]$ and $[0, 1, l]$ correspond to the $T=0$ versions of Figs. 18(d) and 19(b), respectively.

APPENDIX B: SURFACE PHASE DIAGRAMS FOR $d=2$

In the text we have discussed the properties of a two-dimensional surface in contact with a three-dimensional ($d=3$) bulk. Here we describe the case of a one-dimensional surface in contact with a two-dimensional bulk. The key new feature is the absence of all phase transitions from the regions $T > 0, \mu \neq \mu_0$. Away from bulk coexistence, surface behavior is $d-1=1$ dimensional and, thus cannot support¹⁰⁰ phase transitions at $T > 0$. Layer transitions, which persist at $T=0$ only, can be identified by the methods of Sec. II B. Since $T_R=0$ in $d=2$, discrete layer transitions cannot exist at $\mu=\mu_0$, so the only transitions possible at coexistence are of the critical-wetting and critical-drying types. We therefore expect phase diagrams as shown in Fig. 24. Since the $T=0$ transitions can all be calculated exactly, the only parameters of the phase diagram which are not in general exactly calculable are T_c and T_W or T_D .

For the simple example of nearest-neighbor-only interactions [Eq. (8)], the lattice gas is equivalent to the $d=2$ nearest-neighbor $s = \frac{1}{2}$ Ising model, so

$$k_B T_c / |v| = \frac{1}{2 \ln(1 + \sqrt{2})}. \quad (\text{B1})$$

Furthermore, T_W (and by symmetry T_D) has been

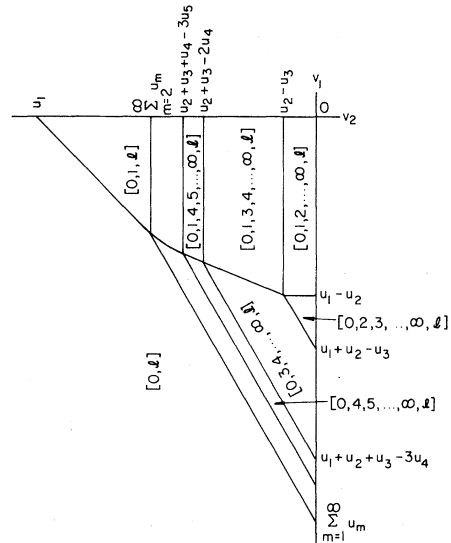


FIG. 23. $T=0$ layer sequencing for nearest- and next-nearest-neighbor attractive atom-atom interactions. When $v_2=0$, the sequences of Fig. 22 are recovered. Nonzero v_2 allows the new sequences, $[0, 1, l]$ and $[0, 1, n, n+1, \dots, \infty, l]$ with $n > 2$.

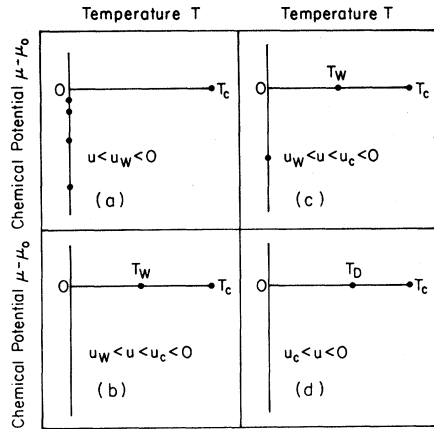


FIG. 24. Surface phase diagrams for $d=2$. There are no transitions at $T > 0$ for $\mu \neq \mu_0$. (a) Strong substrate, showing $T=0$ layer transitions; (b) and (c) Intermediate substrates, showing critical wetting on the coexistence axis. One or more layer transitions may remain on the $T=0$ axis, if the first few layer potentials are strong. (d) Weak substrate, showing critical drying.

calculated exactly⁶¹ and satisfies

$$e^x \left[\cosh x - \cosh \left(x - \frac{2u_1 x}{v} \right) \right] = \sinh x, \quad x = \frac{|v|}{2k_B T}. \quad (\text{B2})$$

The full phase diagram is shown in Fig. 25 (exact), which should be compared with the corresponding $d=3$ picture, Fig. 6. Note the division of the coexistence plane into regions by the critical-wetting and critical-drying lines, as in Fig. 10 (only here $T_R=0$). Because the interactions are nearest neighbor, there is only a single separated layer transition at $T=0$ in

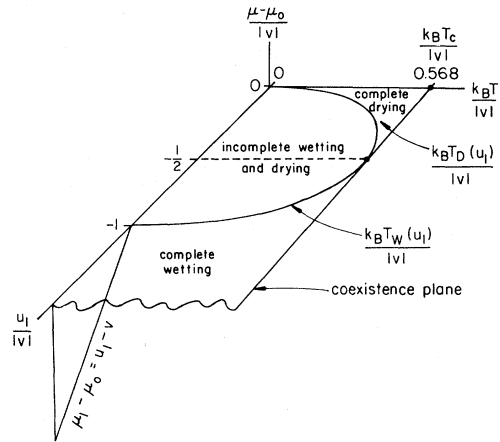


FIG. 25. Exact phase diagram for $d=2$ with nearest-neighbor-only interactions (Ref. 61). There is only one layer transition separated off at $T=0$. The wetting-drying transition curve is given by Eq. (B2). $u_c = v/2$, $u_W = v$.

the strong-substrate regime.

A closely related class of models consists of a structureless (i.e., zero-width) interface bound to a flat surface by a potential well. The wetting (or drying) transition corresponds to thermal unbinding of the interface from the well. These solid-on-solid models can be exactly solved in $d=2$ (one-dimensional interface), where they lead¹⁰¹⁻¹⁰⁵ to a number of interesting results, including $n_s(T, \mu_0^-) \sim 1/(T_W - T)$ as $T \rightarrow T_W^-$. Such models should provide a good physical description of the wetting transition, provided $T_W \ll T_c$. Similar models in $d=3$ promise to be useful in studying phenomena which involve both wetting and roughening.

*Present address: Laboratory of Atomic and Solid State Physics, Clark Hall, Cornell University, Ithaca, N.Y. 14853.

¹J. G. Dash, *Films on Solid Surfaces* (Academic, New York, 1975); A. Thomy, X. Duval, and J. Regnier, *Surf. Sci. Rep.* **1**, 1 (1981).

²*Phase Transitions in Surface Films*, edited by J. G. Dash and J. Ruvalds (Plenum, New York, 1980).

³M. Bienfait, in *Current Topics in Materials Science*, edited by E. Kaldis (North-Holland, New York, 1979); W. A. Steele, *The Interaction of Gases with Solid Surfaces* (Pergamon, Oxford, 1974), Chap. 5.

⁴*Ordering in Two Dimensions*, edited by S. K. Sinha (North-Holland, New York, 1980).

⁵M. J. de Oliveira and R. B. Griffiths, *Surf. Sci.* **71**, 687 (1978).

⁶C. Ebner and W. F. Saam, *Phys. Rev. Lett.* **38**, 1486 (1977).

⁷M. E. Fisher and G. Caginalp, *Commun. Math. Phys.* **56**, 11 (1977).

⁸G. Caginalp and M. E. Fisher, *Commun. Math. Phys.* **65**, 247 (1979).

⁹This language applies, strictly speaking, only to the lattice-gas model of Sec. II. For real, continuum adsorption the layering subregion is not present and the triple-point temperature T_t may play the role of T_R . See discussion in Sec. IV.

¹⁰Under typical experimental conditions the bulk-gas density n_b is small and it is isotherms of $N_{\text{tot}}/A_{\text{tot}}$ which are measured (Ref. 1). The distinction between these isotherms and those involving n_s becomes important when n_b is large (e.g., near the critical point) or

- when n_s is small (e.g., for weak substrates and low temperatures).
- ¹¹J. G. Dash, Phys. Rev. B **15**, 3136 (1977); J. Phys. (Paris), Colloq. **38**, C4-201 (1977).
- ¹²W. A. Zisman, Adv. Chem. **43**, 1 (1963). See also L. D. Landau and E. M. Lifshitz, *Statistical Physics* (Pergamon, Oxford, 1980), pp. 529–533.
- ¹³J. W. Cahn, J. Chem. Phys. **66**, 3667 (1977).
- ¹⁴D. E. Sullivan, J. Chem. Phys. **74**, 2604 (1981).
- ¹⁵D. E. Sullivan, Faraday Symp. Chem. Soc. (in press).
- ¹⁶B. Widom, Faraday Symp. Chem. Soc. (in press).
- ¹⁷G. F. Teletzke, L. E. Scriven, and H. T. Davis (unpublished).
- ¹⁸The statement is precise for nearest-neighbor interactions; however, as we shall see in Sec. III, a finite (generally small) number of layer transitions may continue to extend to $T=0$ in the gas phase for appropriate potentials (e.g., a substrate which is very strong at short distances but much weaker beyond). What is generic is that all remaining transitions (layering or prewetting) terminate at coexistence, on the gas side for $u_w < u < u_c$ and on the liquid side for $u_c < u < 0$.
- ¹⁹Dash defined class III as exhibiting no (measurable) adsorption at coexistence (Ref. 11). In this definition, there is no distinction in principle between a system which is “strongly” class II (finite adsorption) and one which is class III. More recent comments on class III appear in J. G. Dash and R. Peierls, Phys. Rev. B **25**, 5523 (1982). We prefer (Sec. IIC) to distinguish only two types of gas-phase isotherms, infinite adsorption (class I) and finite adsorption (class II) at coexistence. An alternative approach is taken by Sullivan (Refs. 14, 15, and 23), who classifies the behavior of the contact angle at coexistence. Sullivan’s class-II and class-III systems both have finite adsorption on gas-phase isotherms at coexistence.
- ²⁰Note that T_w depends on u , while T_R is strictly an interfacial quantity, independent of u .
- ²¹In the original papers (Refs. 6 and 13), neither Ebner and Saam nor Cahn observed critical wetting, although their models would appear to encompass this possibility, at least for appropriate potentials. Sullivan (Ref. 14), on the other hand, finds *only* critical wetting and no prewetting. A careful study of the nearest-neighbor case by Pandit and Wortis (Ref. 71) reveals critical wetting near enough u_c but changing over to prewetting further from u_c . We believe that this is the general situation, at least within the mean-field context. See Sec. IIC.
- ²²Here again the language applies precisely to the lattice gas (Sec. II). Real adsorbates have three bulk phases. The influence of gas-solid coexistence and the triple point is discussed in Sec. IV.
- ²³D. E. Sullivan, Phys. Rev. B **20**, 3991 (1979). This important paper first sets forth the basic division into strong-, intermediate-, and weak-substrate systems within the context of a continuum mean-field (van der Waals) model. Because of the continuum restriction, layering phenomena cannot be treated. The distinction between the layering, prewetting, and critical-wetting subregions of intermediate substrates is absent.
- ²⁴C. Ebner, Phys. Rev. A **22**, 2776 (1980).
- ²⁵C. Ebner, Phys. Rev. A **23**, 1925 (1981).
- ²⁶J. W. White, R. K. Thomas, T. Trewern, I. Marlow, and G. Bomchil, Surf. Sci. **76**, 13 (1978).
- ²⁷J. Menaucourt, Ph.D. thesis, Université de Nancy, 1977 (unpublished). See especially pp. 86–90.
- ²⁸J. Menaucourt, A. Thomy, and X. Duval, J. Phys. (Paris), Colloq. **38**, C4-195 (1977). This paper contains the surprising (and we believe mistaken) statement, “Presumably... [the number of layer transitions]... increases again below a definite temperature (lower or much lower than 77 K).” This would indicate a return towards class-I behavior at low temperature, contrary to any evidence of which we are aware.
- ²⁹Additional data on intermediate-substrate systems is included in Y. Lahrer and D. Haranger, Surf. Sci. **39**, 100 (1973) and A. Enault, Ph.D. thesis, Université de Nancy, 1975 (unpublished). The authors study Kr and NO on CaI_2 . Both systems show increased layering as T is raised.
- ³⁰M. Wortis, R. Pandit, and M. Schick, in *Melting, Localization, and Chaos*, edited by R. Kalia and P. D. Vashishta (North-Holland, New York, 1982).
- ³¹Possible nonadditivity of van der Waals forces and the influence of this on adsorption has been discussed by I. E. Dzyaloshinskii, E. M. Lifshitz, and L. P. Pitaevskii, Adv. Phys. **10**, 165 (1961).
- ³²See, for example, R. B. Griffiths, in *Phase Transitions and Critical Phenomena*, edited by C. Domb and M. S. Green (Academic, New York, 1972), Vol. 1, p. 7. The contribution of R. B. Griffiths to Ref. 2 (pp. 1ff) contains a particularly cogent account of surface thermodynamics.
- ³³The lattice gas (3) has an imposed lattice structure and is not spatially isotropic, as a real fluid would be. The lattice-gas “liquid” phase is like a real liquid in being high density but like a solid in lacking isotropy. This point is discussed further in Sec. IV.
- ³⁴Technically, this can be done by requiring appropriate boundary conditions, which fix the bulk liquid and gas densities far from the interface, $n(z=-\infty)=n_b^{(g)}$, $n(z=\infty)=n_b^{(l)}$.
- ³⁵Real interactions have a repulsive core; however, in the spirit of the lattice-gas model we may imagine placing the $n=1$ layer at the minimum of the atom-substrate potential and fixing the nearest-neighbor lattice spacing at the minimum of the atom-atom potential. This typically renders all interactions purely attractive.
- ³⁶Convexity in μ is always a property of $f_b(T, \mu)$. It is *not* true in general for $f_s(T, \mu)$ (see Ref. 7). Even at $T=0$ convexity of f_s fails when the full range $-\infty < \mu < \infty$ is included. For $T > 0$ convexity cannot be relied upon except when $n_s \gg n_b$.
- ³⁷We shall always assume that the potentials die off sufficiently rapidly at large distances so that sums such as

- $\sum_m^\infty u_m$ and $\sum_m^\infty mv_m$ are convergent.
- ³⁸A. Thomy and X. Duval, *J. Chim. Phys.* **67**, 286 (1970).
- ³⁹See Appendix B.
- ⁴⁰*Contact Angle, Wettability, and Adhesion*, edited by R. F. Gould (American Chemical Society, Washington, D.C., 1964).
- ⁴¹A. W. Adamson, *Physical Chemistry of Surfaces* (Wiley, New York, 1976).
- ⁴²B. Widom, *J. Chem. Phys.* **62**, 1332 (1975), proposed a general set of triangle inequalities for the interfacial tensions of three coexisting fluid phases. Our Eq. (36) is equivalent to his result in the limiting case that one of the three phases becomes the substrate. He did not at that time include the possibility of strict equality, corresponding to complete wetting or drying.
- ⁴³R. Peierls, *Phys. Rev. B* **18**, 2013 (1978).
- ⁴⁴M. Wortis (unpublished).
- ⁴⁵“Wet” and “not wet” would have been simpler and probably preferable terminology; however, the waters have been muddied by widespread inconsistency in the literature. For example, Cahn (Ref. 13) calls complete wetting “perfect wetting.” Note also in this connection that, for μ strictly less than μ_0 , n_s is always finite and all films are flat everywhere away from surface phase boundaries.
- ⁴⁶Even for purely attractive substrates, it is quite possible to have $n_s < 0$. This happens when atom-atom attractions are strong enough to pull adatoms away from the substrate. Indeed, the methods of Ref. 7 may be used to prove that $n_s < 0$ provided $u_n > \frac{1}{2} \sum_{m=n}^\infty v_m$ for all n .
- ⁴⁷It would presumably be possible artificially to force $n_s \rightarrow -\infty$ in the gas phase by applying a sufficiently long-ranged repulsive substrate potential. This is quite different from the mechanism for $n_s \rightarrow \infty$, which can occur for entirely short-ranged forces. An equivalent remark applies to $n_s \rightarrow \infty$ on the liquid-phase side of coexistence.
- ⁴⁸This picture is reasonable and widely accepted; however, we are aware of no first-principles proof that it is actually what happens in any specific system or model.
- ⁴⁹Of course, in a more general case γ_{gs} and γ_{ls} would depend on the orientation of the substrate surface and the overlayer lattice.
- ⁵⁰G. Antonov, *J. Chim. Phys.* **5**, 372 (1907).
- ⁵¹G. Wulff, *Z. Kristallogr.* **34**, 449 (1901); C. Herring, *Phys. Rev.* **82**, 87 (1951).
- ⁵²W. L. Winterbottom, *Acta Metall.* **15**, 303 (1967); H. Sato and S. Shinozaki, *Surf. Sci.* **22**, 229 (1970).
- ⁵³This parametrization in terms only of the film thickness t neglects interfacial width and variation of film density. Consistency requires that t be much larger than both the coherence length ξ and the potential ranges.
- ⁵⁴The last term in Eq. (41) reflects the fact that interactions across the interface are cut off due to the finite thickness of the film. It costs less free energy to build an interface near a surface than to build one deep in the bulk.
- ⁵⁵(a) The role of long-range forces in controlling film thickness has been discussed recently by P. G. de Gennes, *J. Phys. (Paris) Lett.* **42**, L377 (1981). Renormalization of the effective potentials for $T > T_R$ may modify the $T=0$ power laws found here, as we discuss in Sec. II C 2. (b) S. M. Foiles and N. W. Ashcroft, *Phys. Rev. B* **25**, 1366 (1982); P. Tarazona and R. Evans (unpublished).
- ⁵⁶D. Beaglehole, *J. Chem. Phys.* **73**, 3366 (1980); **75**, 1544 (1981). Reference 16 contains additional references.
- ⁵⁷M. R. Moldover and J. W. Cahn, *Science* **207**, 1073 (1980).
- ⁵⁸R. B. Heady and J. W. Cahn, *J. Chem. Phys.* **58**, 896 (1973).
- ⁵⁹D. E. Sullivan, D. Levesque, and J. J. Weis, *J. Chem. Phys.* **72**, 1170 (1980).
- ⁶⁰N. N. Avgul, G. I. Berezin, A. V. Kisilev, and I. A. Lygina, *Izv. Akad. Nauk. SSSR, Otd. Khim. Nauk.* **2**, 205 (1961).
- ⁶¹D. B. Abraham, *Phys. Rev. Lett.* **44**, 1165 (1980). Abraham refers to the wetting transition as a “roughening transition.” It is more appropriate to think of it as a transition in which the interface unbinds from the surface. In $d=2$ the unbound interface is always rough.
- ⁶²The argument here is physical, based on the fact that nothing “special” happens in the *gas* phase at coexistence, and certainly does not strictly rule out subtle changes in the form of “coexistence curve” singularities.
- ⁶³N. M. Švrakić and M. Wortis, *Phys. Rev. B* **15**, 396 (1977), which contains additional references.
- ⁶⁴H. van Beijeren, *Phys. Rev. Lett.* **38**, 993 (1977); J. V. José, L. P. Kadanoff, S. Kirkpatrick, and D. R. Nelson, *Phys. Rev. B* **16**, 1217 (1977); V. J. Emery and R. H. Swendsen, *Phys. Rev. Lett.* **39**, 1414 (1977). An introductory discussion of roughening which also provides references to the extensive literature is provided by J. D. Weeks, in *Ordering in Strongly Fluctuating Condensed Matter Systems*, edited by T. Riste (Plenum, New York, 1980).
- ⁶⁵Nearest-neighbor interactions, assumed in Eq. (46), capture the essence of the scaling behavior. Cahn (Ref. 13) used the bulk exponent β in place of the surface exponent β_1 .
- ⁶⁶T. W. Burkhardt and E. Eisenriegler, *Phys. Rev. B* **17**, 318 (1978).
- ⁶⁷This is easy to see for the nearest-neighbor case by transforming to the magnetic variables Eqs. (9) and (10).
- ⁶⁸B. Gilquin [Ph.D. thesis, Université de Nancy, 1979 (unpublished), pp. 90–95, 138, and 144] sees class-I behavior between 55 and 70 K. There is evidence (O. E. Vilches, private communication) that O₂ on graphite is class II at low temperatures (~ 10 K).
- ⁶⁹O. D. Kwon, D. Beaglehole, W. W. Webb, B. Widom,

- J. W. Schmidt, J. W. Cahn, M. R. Moldover, and B. Stephenson Phys. Rev. Lett. **48**, 185 (1982); D. W. Pohl and W. I. Goldburg, *ibid.* **48**, 1111 (1982).
- ⁷⁰This assumes both that (38) and (39) hold strictly enough to include the very delicate roughening singularities and that $\gamma_b(\gamma_{gs})$ is nonsingular at T_R . Both statements are reasonable but nonrigorous.
- ⁷¹R. Pandit and M. Wortis, Phys. Rev. B **25**, 3226 (1982). See also R. Pandit, Ph.D. thesis, University of Illinois, 1982 (unpublished).
- ⁷²For a mean-field-like method which does treat roughening, see J. D. Weeks, Phys. Rev. B **26**, 3998 (1982).
- ⁷³We fully believe that this statement is correct; however, it is worth remarking that for $T_w \approx T_c$ it is numerically difficult to follow the sequence of layer transitions to high order (see R. Pandit, thesis, Ref. 71).
- ⁷⁴Note that this includes $n_s(T, \mu_0^-)$, the densities along the gas side of the coexistence curve, itself, for $T < T_w$ (for $T > T_w$, n_s diverges).
- ⁷⁵Note that there is no reason in principle to rule out overlap between adjacent "fingers."
- ⁷⁶The joining involves a small segment of the coexistence axis, so under high enough magnification it consists of three lines meeting at two close cusps.
- ⁷⁷What we call "isobars" are actually scans at constant μ . Because of (4) these are not curves of constant pressure, even in the perfect-gas regime.
- ⁷⁸Because $T_c(n)$ increases with n in this calculation, there will be isotherms for which the early layers are rounded, while all later ones are sharp.
- ⁷⁹A phase diagram similar to Fig. 16(a) was found in Refs. 5 and 24, while one like Fig. 17(c) was found in Ref. 24 for a weaker potential.
- ⁸⁰I. M. Kim and D. P. Landau, Surf. Sci. **110**, 415 (1981).
- ⁸¹W. F. Saam, Surf. Sci. (in press).
- ⁸²For example, by choosing $|\mu_1|$ very large, it is possible to make $T_c(1)$ as high as you please, while leaving T_R unchanged.
- ⁸³On a graphite substrate the critical temperatures $T_c(n)$ for O₂ (Ref. 68), Kr (Refs. 91–93), and Ar (Ref. 94) for layers, $n=1, 2, \dots$, are, respectively, 60, 60.5, 60.0, and ~ 60 K; 87 and 95 K; and 60, 70.0 and 68.0 K. Thus, for O₂, $T_c(n)$ is substantially constant for the first few layers, although it must eventually decrease at least to the triple-point temperature 54.36 K. For Kr, $T_c(n)$ appears to increase with n , while for Ar the trend is not uniform. The triple points of Ar and Kr are ~ 90 and 116 K, respectively, well above the apparent limit, $\lim_{n \rightarrow \infty} T_c(n)$. Note that layer critical temperatures are not easy to determine with precision experimentally.
- ⁸⁴J. J. Rehr and N. D. Mermin, Phys. Rev. A **7**, 379 (1973).
- ⁸⁵F. P. Buff, R. A. Lovett, and F. H. Stillinger, Phys. Rev. Lett. **15**, 621 (1965).
- ⁸⁶Note that roughening, when it occurs, can take place both at the gas-solid coexistence as in NH₄Cl and C₂Cl₆ [K. A. Jackson *et al.*, J. Crystal Growth **40**, 169 (1977)] and at the solid-liquid coexistence as in He [J. E. Avron *et al.*, Phys. Rev. Lett. **45**, 814 (1980)].
- ⁸⁷W. Klein, D. J. Wallace, and R. K. P. Zia, Phys. Rev. Lett. **37**, 639 (1976); W. Klein, Phys. Rev. B **21**, 5254 (1980).
- ⁸⁸C. Rottman, C. Ebner, and M. Wortis (unpublished).
- ⁸⁹This limitation of the lattice-gas model was pointed out to us by E. H. Hauge.
- ⁹⁰The statements below assume that the wetting and drying curves, Figs. 10 and 11, are not reentrant. It seems likely that this is so for reasonable potentials.
- ⁹¹J. H. Singleton and G. D. Halsey, Jr., J. Phys. Chem. **58**, 330, (1954); **58**, 1011 (1954); Can. J. Chem. **33**, 184 Also, C. F. Prenzlow and G. D. Halsey, Jr., J. Phys. Chem. **61**, 1158 (1957).
- ⁹²A. Thomy and X. Duval, J. Chim. Phys. Physicochim. Biol. **66**, 1966 (1969).
- ⁹³A. Thomy and X. Duval, J. Chim. Phys. Physicochim. Biol. **67**, 286 (1970); **67**, 1101 (1970).
- ⁹⁴Reference 68, especially pp. 96–99, 137, and 145.
- ⁹⁵T. T. Chung and J. G. Dash, J. Chem. Phys. **64**, 1855 (1976). The evidence is not from isotherms but is indirect. We know of no modern isotherm data on the N₂-on-graphite system other than in the submonolayer regime.
- ⁹⁶Sullivan (Ref. 23) predicts that Kr will switch near 32 K.
- ⁹⁷M. Bienfait, J. G. Dash, and J. Stoltenberg, Phys. Rev. B **21**, 2765 (1980).
- ⁹⁸S. Ramesh and J. D. Maynard, Phys. Rev. Lett. **49**, 47 (1982).
- ⁹⁹Violation of (A2) would precipitate a failure of the thermodynamic limit (17).
- ¹⁰⁰Technically speaking, one must require that the forces be sufficiently short ranged. See C. Thompson, in *Phase Transitions and Critical Phenomena*, edited by C. Domb and M. S. Green (Academic, New York, 1972), Vol. 1, p. 177ff.
- ¹⁰¹T. W. Burkhardt, J. Phys. A **14**, L63 (1981).
- ¹⁰²S. T. Chui and J. D. Weeks, Phys. Rev. B **23**, 2438 (1981).
- ¹⁰³J. M. J. van Leeuwen and H. J. Hilhorst, Physica **107A**, 319 (1981).
- ¹⁰⁴J. T. Chalker, J. Phys. A **14**, 2431 (1981).
- ¹⁰⁵M. Vallade and J. Lajzerowicz, J. Phys. (Paris) **42**, 1505 (1981).